FINITE ELEMENT SOLUTION
FOR
THIN SHELLS OF REVOLUTION

by

Z. A. Lu
Graduate Student

J. Penzien
Professor of Civil Engineering

E. P. Popov
Professor of Civil Engineering

University of California
Berkeley

September 1963

ERRATA SHEET

Finite Element Solution for Thin Shells of Revolution, by Z. A. Lu, J. Penzien, and E. P. Popov. Institute of Engineering Research Report SESM 63-3, University of California, Berkeley, September 1963.

p. 12, Fig. 1

$$y = 2\sqrt[4]{3(1-\nu^2)}\cdot\sqrt{\frac{2\tan\alpha}{t}}\sqrt{s} \qquad \text{should read} \qquad y = 2\sqrt[4]{3(1-\nu^2)}\sqrt{\frac{2\tan\alpha}{t}}\sqrt{s}$$

p. 17, Line 1

$$b_{22}\, k_6\,(y_i) \qquad \text{should read} \qquad b_{22}\, k_6\,(y_j)$$

p. 24, Line 9

$$(C_{13} - C_{23} - C_{33} - C_{43})\cdot M_i \qquad \text{should read} \qquad (C_{13} - C_{23} - C_{33} - C_{43})\cdot H_i$$

p. 30, Fig. 3

$$K = \frac{Et^3}{12(1-\nu^2)} \qquad \text{should read} \qquad K = \frac{Et^3}{12(1-\nu^2)}$$

p. 44, Line 1

$$\bar{\delta}_{mi} = -\frac{p_r \cot^2\alpha}{2\,Et\sin\alpha}\left[(2-\nu)s_i^2 + \nu\, s_j^2\right]$$

$$\text{should read} \qquad \bar{\delta}_{mi} = -\frac{p_r \cos^2\alpha}{2\,Et\sin\alpha}\left[(2-\nu)s_i^2 + \nu\, s_j^2\right]$$

p. 64, Ex. 5, Line 7

$$\frac{p_r}{2} \qquad \text{should read} \qquad \frac{p\,a}{2}$$

TABLE OF CONTENTS

FOREWORD

The research described in this report, "Finite Element Solution for Thin Shells of Revolution", was conducted under the supervision and technical responsibility of Joseph Penzien and Egor P. Popov, Professors of Civil Engineering, Division of Structural Engineering and Structural Mechanics, University of California, Berkeley, California and was sponsored by the National Aeronautics and Space Administration under NASA Research Grant No. NsG 274-62. Mr. Z. A. Lu, Graduate Student, was responsible for carrying out the detailed theoretical derivations.

ACKNOWLEDGMENT

The authors wish to express their appreciation and sincere thanks to all those individuals who contributed to the completion of this phase of the general investigation. Assistance of Structural Engineering and Structural Mechanics graduate student, Michael Ting, in several phases of this work was particularly valuable. The authors also acknowledge with gratitude the advice received on the computer program from Professor C. F. Scheffey, Edward Wilson, Ian King, and the Computer Center staff. The careful typing of the final manuscript was done by Mrs. S. Kishi and Mrs. M. Umsted.

Finally, the authors wish to thank the National Aeronautics and Space Administration for the financial assistance which made this investigation possible.

I. INTRODUCTION

Thin shells of revolution are widely used in flight structures and their analysis is of great importance to the design engineer. In such shells for symmetrical loadings and small displacements, the membrane stresses and the corresponding elastic displacements can be readily computed. However, due to the variations in thickness, ring-like reinforcements at openings and junctures with the adjoining shells and/or structures, very important bending stresses develop. The analysis of such stresses may be very complex. In fact, solutions are available only for the few simplest possible shapes of the meridian. Also very few solutions exist for the cases of variable thickness and in some of the solutions which are available, the thickness variation is prescribed for reasons of mathematical expediency. On the other hand, functional and manufacturing requirements often demand arbitrary shape and thickness variation of the shell of revolution. To achieve a practical solution for such a general problem is the primary purpose of this investigation.

This first report of the general investigation confines its attention to the elastic analysis of arbitrary shells of revolution assuming small deformations. A general solution of this problem has been obtained by employing finite elements into which any shell of revolution may be subdivided. The basic finite element is a truncated conical shell. Presentation of the detailed analysis of element flexibility, joint loads, matrix solution of the problem, and examples solved with the aid of IBM 7090 computer form the basis of this report. The developed procedures are quite general and can be applied to any symmetrically loaded

shell of revolution. This includes possible variations in shell thickness as well as boundary conditions.

In the second (next) report, the elastic analysis reported here will be extended to include large deformations of the shell. This will be done using a step-by-step procedure. Loads can be applied in small increments and corrected geometry of the shell can be used in each step. It is anticipated that the second report of this series will be followed by another one in which inelastic properties of the material will be incorporated into the analysis as far as possible.

II. REVIEW OF MATHEMATICAL FORMULATIONS

A search of literature shows that the general problem of axi-symmetrically loaded shells of revolution has not been completely solved for the case of arbitrary shape and thickness, non-elastic material and large deformations. However, governing differential equations have been formulated and solutions are available for certain special cases with elastic materials. These will be summarized below.

H. Reissner and Meissner first formulated the governing equations of shells of revolution based on the classical theory of elasticity which can be easily found in Flügge's book on shells[1].

$$\frac{r_2}{r_1}\chi'' + \left[\frac{r_2}{r_1}\cot\phi + \left(\frac{r_2}{r_1}\right)' + \frac{r_2}{r_1}\frac{K'}{K}\right]\chi'$$

$$- \left[\frac{r_1}{r_2}\cot^2\phi + \nu - \nu\frac{K'}{K}\cot\phi\right]\chi = \frac{r_2 r_2 Q_\phi}{K} \qquad (A)$$

$$\frac{r_2}{r_1}(r_2 Q_\phi)'' + \left[\frac{r_2}{r_1}\cot\phi + \left(\frac{r_2}{r_1}\right)' - \frac{r_2}{r_1}\frac{D'}{D}\right](r_2 Q_\phi)'$$

$$- \left[\frac{r_1}{r_2}\cot^2\phi - \nu - \nu\frac{D'}{D}\cot\phi\right](r_2 Q_\phi) = -D(1-\nu^2)r_1\chi + P_g(\phi)$$

where $K = \dfrac{Eh^3}{12(1-\nu^2)}$, $D = \dfrac{Eh}{1-\nu^2}$

Timoshenko in his book gives also the same relations using somewhat different notations[2].

The general procedure of solving Equations (A) consists of eliminating

one or the other of the dependent variables and forming an uncoupled fourth order differential equation. Such an equation is then split, if possible, into two second order differential equations which are then solved. Alternatively, an asymptotic or numerical procedures are used to obtain a solution.

For thin spherical shells of constant thickness, the Reissner-Meissner equations (A) can be solved exactly by the use of hypergeometric series[1][2]; and Zagustin and Young solution[3] using asymptotic integration gives good results for all regions of the shell.

For variable thickness, splitting the two fourth order differential equations into second order equations can be achieved under certain conditions[1]. But asymptotic methods are necessary in general. Rygol[4] solved the resulting asymptotic differential equation in the form $Q_\phi''' + 4\lambda^4 Q_\phi = 0$ by approximating the thickness function λ with two constants. The solution is exact for certain variation of thickness. Kovalenko[5] solved the problem of conical shells of linearly variable thickness when the thickness increases toward the apex.

When the deformations increase, the problem becomes more complicated. E. Reissner[6][7] formulated the governing equations for the case of small deformation but arbitrary rotation as follows.

$$\beta'' + \frac{(rD/\alpha)'}{(rD/\alpha)}\beta' - \left(\frac{\alpha}{r}\right)^2 \cos(\phi+\beta)\left[\sin(\phi+\beta) - \sin\phi\right]$$

$$+ \nu\frac{\alpha}{r}\frac{D'}{D}\left[\sin(\phi+\beta) - \sin\phi\right] + \frac{\nu\alpha}{r}\left[\cos(\phi+\beta) - \cos\phi\right]\phi'$$

$$= \frac{\alpha^2}{rD}\left[\psi \sin(\phi+\beta) - rV\cos(\phi+\beta)\right]$$

$$\psi'' + \frac{(r/C\alpha)'}{(r/C\alpha)}\psi' - \left\{\frac{\alpha^2}{r^2}\cos^2(\phi+\beta) - \frac{\nu\alpha}{r}\left[\sin(\phi+\beta)(\phi'+\beta') + \frac{C'}{C}\cos(\phi+\beta)\right]\right\}\psi = \frac{\alpha^2 C}{r}\left[\cos(\phi+\beta) - \cos\phi\right]$$

$$+ \frac{\nu\alpha}{r}\sin(\phi+\beta)(rV)' + \left\{\frac{\alpha^2}{r^2}\sin(\phi+\beta)\cos(\phi+\beta) + \frac{\nu\alpha}{r}\left[\cos(\phi+\beta)(\phi'+\beta') - \frac{C'}{C}\sin(\phi+\beta)\right]\right\}(rV) - \frac{\alpha}{r}(r^2 p_H)'$$

$$- \left[\nu\frac{\alpha^2}{r^2}\cos(\phi+\beta) - \frac{\alpha}{r}\frac{C'}{C}\right](r^2 p_H) \qquad \text{(B)}$$

where $D = \dfrac{Eh^3}{12(1-\nu^2)}$ $\qquad C = Eh$

By expanding in series

$$\cos(\phi+\beta) = \cos\phi - \beta\sin\phi - \frac{\beta^2}{2!}\cos\phi \ .....$$

$$\sin(\phi+\beta) = \sin\phi + \beta\cos\phi - \frac{\beta^2}{2!}\sin\phi \ .....$$

and retaining only powers up to, or in certain expressions, lower than β^2 he obtained the "small finite deflection theory". The governing equations become

$$\beta'' + \frac{(rD/\alpha)'}{(rD/\alpha)}\beta' - \left[\left(\frac{r'}{r}\right)^2 - \nu\frac{(r'D/\alpha)'}{(rD/\alpha)}\right]\beta + \left[\frac{3}{2}\frac{r'z'}{r^2} - \frac{\nu}{2}\frac{(z'D/\alpha)'}{(rD/\alpha)}\right]\beta^2$$

$$= \frac{\alpha^2}{rD}\left\{\psi\sin\phi - (rV)\cos\phi + \left[\psi\cos\phi + (rV)\sin\phi\right]\beta\right\}$$

$$\psi'' + \frac{(r/C\alpha)'}{(r/C\alpha)}\psi' - \left[\left(\frac{r'}{r}\right)^2 + \nu\frac{(r'/C\alpha)'}{(r/C\alpha)}\right]\psi \qquad \text{(B-a)}$$

$$+ \left[2\frac{z'r'}{r^2} + \nu\frac{(z'/C\alpha)'}{(r/C\alpha)}\right]\beta\psi + \nu\frac{z'}{r}\beta'\psi = -\frac{\alpha^2 C}{r}\left[\beta\sin\phi + \frac{\beta^2}{2}\cos\phi\right] + \left[\frac{z'r'}{r^2} + \nu\frac{(z'/C\alpha)'}{(r/C\alpha)}\right](rV) + \nu\frac{z'}{r}(rV)'$$

$$+\left[\frac{r'^2-z'^2}{r^2}+\nu\frac{(r'/C\alpha)'}{(r/C\alpha)}\right]\beta\,(rV)+\nu\frac{r'}{r}\beta'\,(rV)+\nu\frac{r'}{r}\beta\,(rV)'$$

$$-\frac{\alpha}{r}(r^2p_H)'-\left[\nu\left(\frac{\alpha r'}{r^2}-\frac{\alpha z'}{r^2}\beta\right)-\frac{\alpha}{r}\frac{C'}{C}\right](r^2p_H)$$

For the general case, a solution of these equations is very difficult. But for special cases (cylinders, spheres) with constant thickness, asymptotic solutions are possible.

If only the linear terms are retained, the above equations further simplify into those corresponding to the "small deformation theory", different form from that given by (A). The equations take the following form:

$$\beta''+\frac{(rD/\alpha)'}{(rD/\alpha)}\beta'-\left[\left(\frac{r'}{r}\right)^2-\nu\frac{(r'D/\alpha)'}{(rD/\alpha)}\right]\beta=\frac{z'}{(rD/\alpha)}\psi-\frac{r'}{(rD/\alpha)}(rV)$$

$$\psi''+\frac{(r/C\alpha)'}{(r/C\alpha)}\psi'-\left[\left(\frac{r'}{r}\right)^2+\nu\frac{(r'/C\alpha)'}{(r/C\alpha)}\right]\psi=-\frac{z'}{(r/C\alpha)}\beta$$

$$+\left[\frac{z'r'}{r^2}+\nu\frac{(z'/C\alpha)'}{(r/C\alpha)}\right](rV)+\nu\frac{z'}{r}(rV)' \qquad \text{(B-b)}$$

$$-\left[\frac{(r/C\alpha)'}{(r/C\alpha)}+\nu\frac{r'}{r}\right](r\alpha p_H)-(r\alpha p_H)'$$

The solution possibility of this set has been discussed before.

Naghdi and De Silva[8][9][10] did some work in detail on E. Reissner's equation. Their solution process made use of complex auxiliary functions and Langer's method of asymptotic integration[11].

Further complication arises when the effect of transverse shear deformation is considered. Following E. Reissner's formulation for small deformations Naghdi[12][13] included transverse shear deformation and derived the following equations for general axi-symmetrical shells of revolution.

$$\beta'' + \left[(1 - k\lambda^2)\frac{(rD/\alpha)'}{(rD/\alpha)} - k\lambda\left(2\lambda' + \frac{k'}{k}\lambda\right)\right]\beta' - \left\{(1 - k\lambda^2)\left[\left(\frac{r'}{r}\right)^2 - \nu\frac{(r'D/\alpha)'}{(rD/\alpha)}\right] + \nu k\lambda\left(2\lambda' + \frac{k'}{k}\lambda\right)\left(\frac{r'}{r}\right)\right\}\beta$$

$$= \frac{z'}{(rD/\alpha)}\psi - \frac{r'}{(rD/\alpha)}(rV) + \left(\frac{\lambda}{C}\right)\left\{-\left[(r'H)' - \nu\psi''\right] - \left[\frac{(\lambda/C)'}{(\lambda/C)} + \frac{(rD/\alpha)'}{(rD/\alpha)} - \nu\left(\frac{r'}{r}\right)\right](r'H) + \left[\nu\frac{(\lambda/C)'}{(\lambda/C)} + \nu\frac{(rD/\alpha)'}{(rD/\alpha)} + \left(\frac{r'}{r}\right)\right]\psi'\right\} + \left(\frac{\lambda}{C}\right)\left\{\left[(z'V)' - \nu(r\alpha p_H)'\right] + \left[\frac{(\lambda/C)'}{(\lambda/C)} + \frac{(rD/\alpha)'}{(rD/\alpha)} - \nu\left(\frac{r'}{r}\right)\right](z'V) - \left[\nu\frac{(\lambda/C)'}{(\lambda/C)} + \nu\frac{(rD/\alpha)'}{(rD/\alpha)} - \left(\frac{r'}{r}\right)\right](r\alpha p_H)\right\} \qquad (C)$$

$$\psi'' + \frac{(r/C\alpha)'}{(r/C\alpha)}\psi' - \left[\left(\frac{r'}{r}\right)^2 + \nu\frac{(r'/C\alpha)'}{(r/C\alpha)}\right]\psi = -\frac{z'}{(r/C\alpha)}\beta - \frac{k\lambda}{(r/C\alpha)}\left\{\nu\left(\frac{r}{\alpha}\right)\beta'' + \left[2\left(\frac{r'}{\alpha}\right) + \nu\left(\frac{r}{\alpha}\right)' + \nu\left(\frac{r}{\alpha}\right)\frac{(k\lambda)'}{(k\lambda)}\right]\beta' + \left[\left(\frac{r}{\alpha}\right)\left(\frac{r'}{r}\right)' + \left(\frac{r'}{\alpha}\right)\left(\frac{r'}{r}\right) + \nu\left(\frac{r'}{\alpha}\right)\left(\frac{r'}{r}\right) + \left(\frac{r'}{\alpha}\right)\frac{(k\lambda)'}{(k\lambda)}\right]\beta\right\} + \left[\frac{z'r'}{r^2} + \nu\frac{(z'/C\alpha)'}{(r/C\alpha)}\right](rV) + \nu\frac{z'}{r}(rV)' - \left[\frac{(r/C\alpha)'}{(r/C\alpha)} + \nu\frac{r'}{r}\right](r\alpha p_H) - (r\alpha p_H)' - \frac{z'}{(r/C\alpha)}\gamma^{o}_{\xi 5}$$

(Note: $\psi = rH$) $\qquad k = \dfrac{h^2}{12(1-\nu^2)}$

If we set λ and $\gamma_{\xi 5} = 0$, the equations reduce to (B-b).

The solution procedure for these equations is much the same as that used earlier by Naghdi for the case without transverse shear effect.

For large deformations and non-linear material, solution can be found only for membrane theory with isotropic incompressible material[17].

Since the available mathematical solutions are extremely complex and since it is almost impossible to incorporate into these solutions

the general practical range of shells with regard to shape, thickness, material, and magnitude of deformations, an approximate, stepwise, pseudo-elastic finite element solution has been formulated. In a general problem, the actual shell of revolution is considered to be an assemblage of a large number of straight cones each of uniform thickness with the exception of the top (or bottom) element which is a shallow spherical cap of its own uniform thickness. Loads can be applied in small increments for investigations of large deformations and/or inelastic behavior of material. For each step of loading the displacements of the nodal points and the forces in the conical and spherical elements can be calculated by standard matrix operations. The displacements of the nodal points define a new geometry of the assemblage and hence new geometry and structural properties of each element. From the forces in the elements the stresses and strains can be computed which determine whether or not a new set of constants defining the material properties should be assigned to each element for the next increment of load. In this manner, the problems of large deformation and change of material properties after yielding will be treated in subsequent reports. How the material properties vary under biaxial stress conditions is the subject of a separate experimental investigation. By making the size of elements and the load increments sufficiently small, the actual case of smoothly varying shape and thickness as well as gradual yielding of material can be approximated. This report is confined, however, only to the analysis of one load application, i.e., the reported solution is complete for axi-symmetrical loading of an arbitrary elastic shell of revolution experiencing small displacements.

III. THEORY OF FINITE ELEMENT SOLUTION

A. General Procedure.

The basic principles and procedures employed in the applications of the finite element method in structural analysis for the case of small deformations and elastic material have become well known in recent years and are described in several publications[18][19][20]. The basic steps consist of:

(1) Establishing the stiffness of the structure from the stiffness (or flexibility) of the individual elements,

(2) Calculation of the forces on or the displacements of the joints of the structure, and

(3) Calculation of the forces and deformations of the elements.

In Step (1), some matrices defining the geometrical relations between the structure and the elements are used.

In the ordinary structural problems the element flexibilities are symmetrical with respect to the main diagonal and only three quantities are required to solve the problem completely. These quantities are:

(1) Element stiffness matrix which includes the stiffness of all elements in a diagonal arrangement,

(2) Loads or displacements imposed on the joints of the structure, and

(3) The displacement transformation matrix.

However, in the problem considered here, element forces per unit length are involved and hence unsymmetrical flexibility or stiffness matrices is obtained. Therefore, another geometrical matrix which will be called

the "equilibrium matrix" is required in addition to the displacement transformation matrix. Each of these quantities will be discussed in detail in subsequent sections.

B. Element Flexibilities

1. Conical Segment. The displacements of the edges of a conical ring due to forces (including moments) applied on the edges can be obtained from mathematical solutions for conical shells. The expressions derived by Flügge[1] will be used as the basis of our formulation.

Flügge's bending solution of conical shell yields the following relations.

$$
\begin{aligned}
Q_s &= \frac{1}{s}\Big[A_1(\text{ber } y - 2y^{-1}\,\text{bei}'y) + A_2(\text{bei } y + 2y^{-1}\,\text{ber}'y) \\
&\quad + B_1(\text{ker } y - 2y^{-1}\,\text{kei}'y) + B_2(\text{kei } y + 2y^{-1}\,\text{ker}'y)\Big] \\
N_s &= -Q_s \cot\alpha \\
N_\theta &= -\frac{\cot\alpha}{2s}\Big[A_1(y\,\text{ber}'y - 2\,\text{ber } y + 4y^{-1}\,\text{bei}'y) \\
&\quad + A_2(y\,\text{bei}'y - 2\,\text{bei } y - 4y^{-1}\,\text{ber}'y) \\
&\quad + B_1(y\,\text{ker}'y - 2\,\text{ker } y + 4y^{-1}\,\text{kei}'y) \\
&\quad + B_2(y\,\text{kei}'y - 2\,\text{kei } y - 4y^{-1}\,\text{ker}'y)\Big] \\
M_s &= 2y^{-2}\Big\{A_1\Big[y\,\text{bei}'y - 2(1-\nu)(\text{bei } y + 2y^{-1}\,\text{ber}'y)\Big] \\
&\quad - A_2\Big[y\,\text{ber}'y - 2(1-\nu)(\text{ber } y - 2y^{-1}\,\text{bei}'y)\Big] \\
&\quad + B_1\Big[y\,\text{kei}'y - 2(1-\nu)(\text{kei } y + 2y^{-1}\,\text{ker}'y)\Big] \\
&\quad - B_2\Big[y\,\text{ker}'y - 2(1-\nu)(\text{ker } y - 2y^{-1}\,\text{kei}'y)\Big]\Big\} \\
M_\theta &= 2y^{-2}\Big\{A_1\Big[\nu y\,\text{bei}'y + 2(1-\nu)(\text{bei } y + 2y^{-1}\,\text{ber}'y)\Big] \\
&\quad - A_2\Big[\nu y\,\text{ber}'y + 2(1-\nu)(\text{ber } y - 2y^{-1}\,\text{bei}'y)\Big] \\
&\quad + B_1\Big[\nu y\,\text{kei}'y + 2(1-\nu)(\text{kei } y + 2y^{-1}\,\text{ker}'y)\Big] \\
&\quad - B_2\Big[\nu y\,\text{ker}'y + 2(1-\nu)(\text{ker } y - 2y^{-1}\,\text{kei}'y)\Big]\Big\}
\end{aligned}
\qquad \text{(I-a)}
$$

$$\chi = \frac{2\sqrt{3(1-\nu^2)}\cot\alpha}{Et^2}\left[A_1\,(\text{bei}\ y + 2y^{-1}\,\text{ber}'y)\right.$$
$$- A_2\,(\text{ber}\ y - 2y^{-1}\,\text{bei}'y) + B_1\,(\text{kei}\ y + 2y^{-1}\,\text{ker}'y)$$
$$\left. - B_2\,(\text{ker}\ y - 2y^{-1}\,\text{kei}'y)\right]$$

Flugge did not give expressions for v and w. But these can be derived from the stress-strain and strain-displacement relations

$$\epsilon_\theta = \frac{1}{Et}(N_\theta - \nu N_s) \quad ; \quad \epsilon_\theta = \frac{1}{Et}(N_s - \nu N_\theta) \qquad \text{(II)}$$

and

$$\epsilon_\theta = \frac{v}{s} + \frac{w\tan\alpha}{s} \quad ; \quad \epsilon_\theta = \frac{dv}{ds}$$

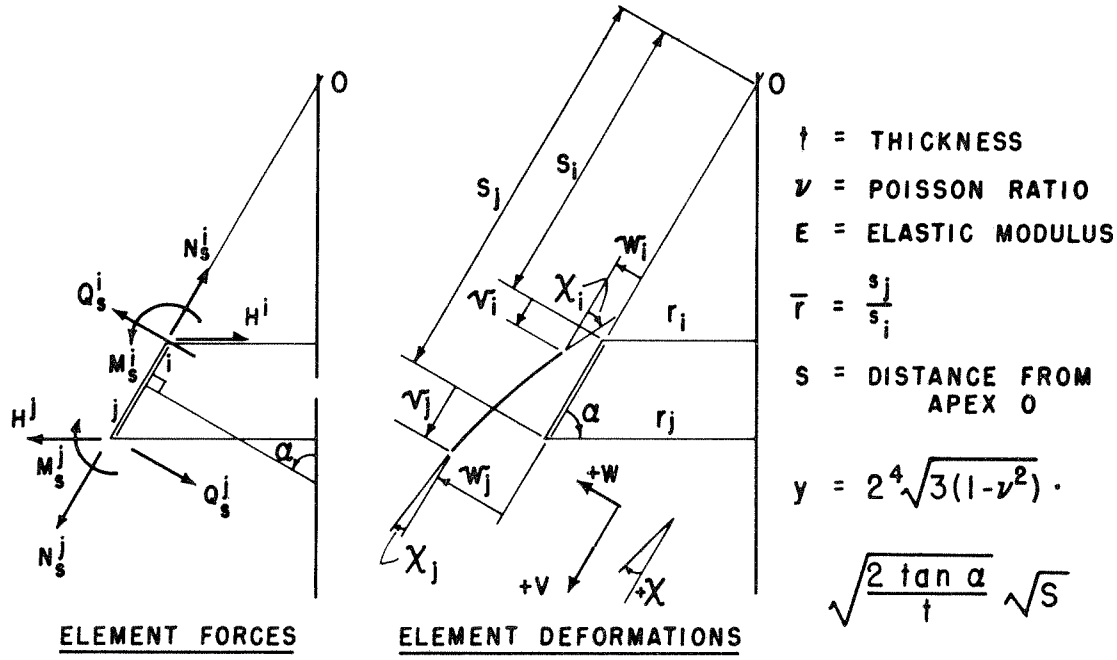

FIG. I - CONICAL ELEMENT

Using the expressions for N_θ and N_s from (I-a), eliminating and integrating (II), we obtain

$$
\begin{aligned}
v = \frac{2\cot\alpha}{Et}\Bigg\{ & A_1\left[\frac{\nu}{2}\,\mathrm{ber}\,y - (1+\nu)y^{-1}\,\mathrm{bei}'y\right] \\
& + A_2\left[\frac{\nu}{2}\,\mathrm{bei}\,y + (1+\nu)y^{-1}\,\mathrm{ber}'y\right] \\
& + B_1\left[\frac{\nu}{2}\,\mathrm{ker}\,y - (1+\nu)y^{-1}\,\mathrm{kei}'y\right] \\
& + B_2\left[\frac{\nu}{2}\,\mathrm{kei}\,y + (1+\nu)y^{-1}\,\mathrm{ker}'y\right]\Bigg\}
\end{aligned}
\qquad \text{(I-b)}
$$

$$
\begin{aligned}
w = \frac{\cot^2\alpha}{Et}\Bigg\{ & A_1\left[\mathrm{ber}\,y - \tfrac{1}{2}\,y\,\mathrm{ber}'y\right] + A_2\left[\mathrm{bei}\,y - \tfrac{1}{2}\,y\,\mathrm{bei}'y\right] \\
& + B_1\left[\mathrm{ker}\,y - \tfrac{1}{2}\,y\,\mathrm{ker}'y\right] + B_2\left[\mathrm{kei}\,y - \tfrac{1}{2}\,y\,\mathrm{kei}'y\right]\Bigg\}
\end{aligned}
$$

In the first of (I-b) integrals of Thompson functions have been removed by using the following identities

$$
\begin{aligned}
&\int_o^y y\,\mathrm{ber}\,y\,dy = y\,\mathrm{bei}'y\ , \qquad \int_o^y y\,\mathrm{bei}\,y\,dy = -y\,\mathrm{ber}'y \\
&\int_o^y y\,\mathrm{ker}\,y\,dy = y\,\mathrm{kei}'y\ , \qquad \int_o^y y\,\mathrm{kei}\,y\,dy = -y\,\mathrm{ker}'y
\end{aligned}
\qquad (1)
$$

The positive directions of the forces and displacements in a conical element are shown in Fig. 1.

It should be noted that Flügge's bending solution of conical shell was obtained from a system in which only horizontal force acts radially at the periphery, the vertical force on the ring is zero. This can be noted from Flügge's comment on the governing differential equation in Ref. (1), and is reflected by the expressions of Q_s and N_s from (I-a), which imply that there is only one force H applied such that

$$
Q_s = -H\sin\alpha\ , \qquad N_s = H\cos\alpha \qquad (2)
$$

The expressions N_s and N_θ given by (I-a) are the resulting membrane forces in the shell due to the application of bending moments and horizontal forces at the edges. If a force N_s is applied at the edge of the ring as a source of disturbance, the induced forces and deformations in the shell cannot be obtained from (I-a) and (I-b) and should be computed from the expressions resulting from a membrane type analysis.

Flügge also gives the solution to the problem of membrane deformation of conical shells[1]. The resulting expressions for the case where no distributed loads are applied to the shell surface are

$$\begin{aligned} v &= \frac{C}{Et} \log s + C_1 \\ w &= -\frac{C}{Et} \cot\alpha \, (\log s + \nu) - C_1 \cot\alpha \\ \chi &= -\frac{C}{Et} \cot\alpha \cdot \frac{1}{s} \end{aligned} \qquad \text{(I-c)}$$

where C and C_1 are constants of integrations to be determined from a force condition and a displacement condition respectively on the boundary.

For the case of zero distributed loads, $C = N_s \cdot s = N_s^i \cdot s_i = N_s^j \cdot s_j$.

It must be pointed out that for equilibrium in the vertical direction a force N_s^j applied at edge j has to be balanced by a force N_s^i applied at edge i . The bending moment or horizontal force applied individually at either edge is self-equilibrating. Membrane deformations can only be computed with respect to some reference position which is governed by the constant C_1 .

To avoid the coupling of bending and membrane actions and for the reason mentioned in the previous paragraph, we choose M_s , H applied at both edges and N_s applied at the lower edge as the basic element

force quantities, and arbitrarily assume that the ring is held stationary at the upper edge during stretch, i.e. $v_i = 0$, under the action of membrane force N_s .

Four boundary conditions define the four constants A_1 , A_2 , B_1 , B_2 of Eq. (I-a). These are

$$\begin{aligned} &\text{at } y = y_i \ , \qquad M_s = M_i \ , \qquad H = H_i \\ &\text{at } y = y_j \ , \qquad M_s = M_j \ , \qquad H = H_j \end{aligned} \tag{3}$$

Upon substituting the expressions of A_1 , A_2 , B_1 , B_2 , which are now functions of M_i , M_j , H_i , H_j into Eqs. (I-a) and (I-b) we obtain the force and deformation quantities as functions of M_i , M_j , H_i , H_j and of Thompson functions and their first derivatives. The algebraic manipulation is lengthy and tedious. Only the resulting expressions in symbolic form will be given below.

Before we present the resulting force and deformation expressions, we need to define a few more quantities.

To correspond with the horizontal force H, there must be a horizontal displacement δ . From simple geometry

$$\delta = w \sin \alpha + v \cos \alpha \tag{4}$$

We see that the positive direction of δ is outward.

We then find that the deformations χ_i , χ_j , δ_i , δ_j as defined by Flügge's solution are not all in the same direction as the corresponding forces M_i , M_j , H_i , H_j . Also since the membrane force N_j and N_i exist simultaneously we must define the corresponding deformation in the same sense. (From now on we abbreviate the symbol N_s^i and N_s^j as N_i and N_j where $N_i = \bar{r} N_j$.) Thus, we introduce the following as the basic element deformation quantities corresponding to the basic

element force quantities we have chosen.

$$\begin{aligned} \bar{\chi}_i &= -\chi_i \\ \bar{\chi}_j &= \chi_j \\ \bar{\delta}_i &= -\delta_i \\ \bar{\delta}_j &= \delta_j \\ e &= v_j - v_i \end{aligned} \tag{5}$$

The deformations as a result of the application of the forces M_i , M_j , H_i , H_j are

$$\begin{aligned} \bar{\chi}_i = -Cp1 \Big\{ & \Big[a_{12}b_2(y_i) - a_{22}b_1(y_i) + b_{12}k_2(y_i) - b_{22}k_1(y_i) \Big] M_i \\ & + \Big[a_{14}b_2(y_i) - a_{24}b_1(y_i) + b_{14}k_2(y_i) - b_{24}k_1(y_i) \Big] M_j \\ & + \Big[a_{11}b_2(y_i) - a_{21}b_1(y_i) + b_{11}k_2(y_i) - b_{21}k_1(y_i) \Big] H_i \\ & + \Big[a_{13}b_2(y_i) - a_{23}b_1(y_i) + b_{13}k_2(y_i) - b_{23}k_1(y_i) \Big] H_j \Big\} \end{aligned}$$

$$\begin{aligned} \bar{\chi}_j = Cp1 \Big\{ & \Big[a_{12}b_2(y_j) - a_{22}b_1(y_j) + b_{12}k_2(y_j) - b_{22}k_1(y_j) \Big] M_i \\ & + \Big[a_{14}b_2(y_j) - a_{24}b_1(y_j) + b_{14}k_2(y_j) - b_{24}k_1(y_j) \Big] M_j \\ & + \Big[a_{11}b_2(y_j) - a_{21}b_1(y_j) + b_{11}k_2(y_j) - b_{21}k_1(y_j) \Big] H_i \\ & + \Big[a_{13}b_2(y_j) - a_{23}b_1(y_j) + b_{13}k_2(y_j) - b_{23}k_1(y_j) \Big] H_j \Big\} \end{aligned}$$

$$\begin{aligned} \bar{\delta}_i = -Cp3 \Big\{ & \Big[a_{12}b_5(y_i) + a_{22}b_6(y_i) + b_{12}k_5(y_i) + b_{22}k_6(y_i) \Big] M_i \\ & + \Big[a_{14}b_5(y_i) + a_{24}b_6(y_i) + b_{14}k_5(y_i) + b_{24}k_6(y_i) \Big] M_j \\ & + \Big[a_{11}b_5(y_i) + a_{21}b_6(y_i) + b_{11}k_5(y_i) + b_{21}k_6(y_i) \Big] H_i \\ & + \Big[a_{13}b_5(y_i) + a_{23}b_6(y_i) + b_{13}k_5(y_i) + b_{23}k_6(y_i) \Big] H_j \Big\} \end{aligned}$$

$$
\begin{aligned}
\bar{\delta}_j = Cp3 \Big\{ & \Big[a_{12} b_5(y_j) + a_{22} b_6(y_j) + b_{12} k_5(y_j) + b_{22} k_6(y_i) \Big] M_i \\
& + \Big[a_{14} b_5(y_j) + a_{24} b_6(y_j) + b_{14} k_5(y_j) + b_{24} k_6(y_j) \Big] M_j \\
& + \Big[a_{11} b_5(y_j) + a_{21} b_6(y_j) + b_{11} k_5(y_j) + b_{21} k_6(y_j) \Big] H_i \\
& + \Big[a_{13} b_5(y_j) + a_{23} b_6(y_j) + b_{13} k_5(y_j) + b_{23} k_6(y_j) \Big] H_j \Big\}
\end{aligned}
$$

$$
\begin{aligned}
e = Cp2 \Big\{ & \Big[a_{12} \big\langle b_9(y_j) - b_9(y_i) \big\rangle + a_{22} \big\langle b_{10}(y_j) - b_{10}(y_i) \big\rangle \\
& + b_{12} \big\langle k_9(y_j) - k_9(y_i) \big\rangle + b_{22} \big\langle k_{10}(y_j) - k_{10}(y_i) \big\rangle \Big] M_i \\
& + \Big[a_{14} \big\langle b_9(y_j) - b_9(y_i) \big\rangle + a_{24} \big\langle b_{10}(y_j) - b_{10}(y_i) \big\rangle \\
& + b_{14} \big\langle k_9(y_j) - k_9(y_i) \big\rangle + b_{24} \big\langle k_{10}(y_j) - k_{10}(y_i) \big\rangle \Big] M_j \\
& + \Big[a_{11} \big\langle b_9(y_j) - b_9(y_i) \big\rangle + a_{21} \big\langle b_{10}(y_j) - b_{10}(y_i) \big\rangle \\
& + b_{11} \big\langle k_9(y_i) - k_9(y_i) \big\rangle + b_{21} \big\langle k_{10}(y_j) - k_{10}(y_i) \big\rangle \Big] H_i \\
& + \Big[a_{13} \big\langle b_9(y_j) - b_9(y_i) \big\rangle + a_{23} \big\langle b_{10}(y_j) - b_{10}(y_i) \big\rangle \\
& + b_{13} \big\langle k_9(y_j) - k_9(y_i) \big\rangle + b_{23} \big\langle k_{10}(y_j) - k_{10}(y_i) \big\rangle \Big] H_j \Big\}
\end{aligned}
\qquad \text{(III-a)}
$$

where $Cp1 = \dfrac{2\sqrt{3(1-\nu^2)}\ \cot\alpha}{Et^2}$, $Cp2 = \dfrac{\cot\alpha}{Et}$, $Cp3 = \dfrac{\cot\alpha \cdot \cos\alpha}{Et}$

$$
a_{11} = -\sin\alpha \cdot s_i \frac{d_{11}}{\Delta} \; ; \quad a_{12} = -\frac{y_i^2}{2}\frac{d_{12}}{\Delta} \; ; \quad a_{13} = -\sin\alpha \cdot s_j \frac{d_{13}}{\Delta} \; ; \quad a_{14} = -\frac{y_j^2}{2}\frac{d_{14}}{\Delta}
$$

$$
a_{21} = \sin\alpha \cdot s_i \frac{d_{21}}{\Delta} \; ; \quad a_{22} = \frac{y_i^2}{2}\frac{d_{22}}{\Delta} \; ; \quad a_{23} = \sin\alpha \cdot s_j \frac{d_{23}}{\Delta} \; ; \quad a_{24} = \frac{y_j^2}{2}\frac{d_{24}}{\Delta}
$$

$$
b_{11} = -\sin\alpha \cdot s_i \frac{d_{31}}{\Delta} \; ; \quad b_{12} = -\frac{y_i^2}{2}\frac{d_{32}}{\Delta} \; ; \quad b_{13} = -\sin\alpha \cdot s_j \frac{d_{33}}{\Delta} \; ; \quad b_{14} = -\frac{y_j^2}{2}\frac{d_{34}}{\Delta}
$$

$$
b_{21} = \sin\alpha \cdot s_i \frac{d_{41}}{\Delta} \; ; \quad b_{22} = \frac{y_i^2}{2}\frac{d_{42}}{\Delta} \; ; \quad b_{23} = \sin\alpha \cdot s_j \frac{d_{43}}{\Delta} \; ; \quad b_{24} = \frac{y_j^2}{2}\frac{d_{44}}{\Delta}
$$

$$\Delta = \begin{vmatrix} b_1(y_i) & b_2(y_i) & k_1(y_i) & k_2(y_i) \\ b_4(y_i) & -b_3(y_i) & k_4(y_i) & -k_3(y_i) \\ b_1(y_j) & b_2(y_j) & k_1(y_j) & k_2(y_j) \\ b_4(y_j) & -b_3(y_j) & k_4(y_j) & -k_3(y_j) \end{vmatrix}$$

d_{ji} = minors of item ij in the determinant Δ.

$$b_1(y) = \text{ber } y - 2y^{-1} \text{ bei}'y$$

$$b_2(y) = \text{bei } y + 2y^{-1} \text{ ber}'y$$

$$k_1(y) = \text{ker } y - 2y^{-1} \text{ kei}'y$$

$$k_2(y) = \text{kei } y + 2y^{-1} \text{ ker}'y$$

$$b_3(y) = y \text{ ber}'y - 2(1-\nu)\, b_1(y)$$

$$b_4(y) = y \text{ bei}'y - 2(1-\nu)\, b_2(y)$$

$$k_3(y) = y \text{ ker}'y - 2(1-\nu)\, k_1(y)$$

$$k_4(y) = y \text{ kei}'y - 2(1-\nu)\, k_2(y)$$

$$b_5(y) = -\tfrac{1}{2}\left[y \text{ ber}'y - 2(1+\nu)\, b_1(y) \right]$$

$$b_6(y) = -\tfrac{1}{2}\left[y \text{ bei}'y - 2(1+\nu)\, b_2(y) \right]$$

$$k_5(y) = -\tfrac{1}{2}\left[y \text{ ker}'y - 2(1+\nu)\, k_1(y) \right]$$

$$k_6(y) = -\tfrac{1}{2}\left[y \text{ kei}'y - 2(1+\nu)\, k_2(y) \right]$$

$$b_9(y) = \nu \text{ ber } y - 2(1+\nu)\, y^{-1} \text{ bei}'y$$

$$b_{10}(y) = \nu \text{ bei } y + 2(1+\nu)\, y^{-1} \text{ ber}'y$$

$$k_9(y) = \nu \text{ ker } y - 2(1+\nu)\, y^{-1} \text{ kei}'y$$

$$k_{10}(y) = \nu \text{ kei } y + 2(1+\nu)\, y^{-1} \text{ ker}'y$$

$$\begin{Bmatrix} A_1 \\ A_2 \\ B_1 \\ B_2 \end{Bmatrix} = \begin{bmatrix} a_{11} & a_{12} & a_{13} & a_{14} \\ a_{21} & a_{22} & a_{23} & a_{24} \\ b_{11} & b_{12} & b_{13} & b_{14} \\ b_{21} & b_{22} & b_{23} & b_{24} \end{bmatrix} \cdot \begin{Bmatrix} H_i \\ M_i \\ H_j \\ M_j \end{Bmatrix} \tag{7}$$

and from (I-c) supplemented by

$$\begin{aligned} C_1 &= -\frac{N_j s_j}{Et} \log s_i \\ N_s &= \frac{N_j s_j}{s} \\ N_\theta &= 0 \end{aligned} \tag{8}$$

Referring back to the shell solutions from which Eq. (6) was developed we see that force quantities are all in units of pounds or pound-inches per unit length. Hence the f matrix so obtained is not symmetrical with respect to the main diagonal. Items of the matrix representing deformations due to forces on the same edge of the ring are symmetrical, while those representing effects of forces across the edges are not. The latter bear a ratio of $\bar{r}$ to each other which reflects the ratio of the circumferences between the two edges of the ring. However, it can be easily shown that items of f matrix do satisfy Betti's law. We could use the total forces around an edge as basic force quantities and obtain a symmetrical f matrix. But since at later stages we shall make frequent use of the expressions from shell solutions which involve forces per unit length, we choose to retain its present form.

The accuracy of the f matrix, judged from the values of the quantities on opposite sides of the main diagonal, has been investigated

over a wide range of thickness, lengths, angles and radii of cones. It was found that the first 4x4 portion is nearly perfect for almost any case provided the length of the element is not smaller than the thickness, but the fifth column and fifth row which depend on different mathematical functions diverge more and more as the geometry of the cone approaches extreme cases. The first 4x4 submatrix, representing entirely the bending effect, is valid as long as tan α is finite, but discrepancies between items on opposite sides of the diagonal increase as α approaches 90°; in such cases the expressions for cylindrical shells should be used. To reduce discrepancies between quantities of the fifth column and the fifth row, it is recommended that for $\alpha < 30^{\circ}$ (since for small α plate action predominates) quantities of the fifth row be used to establish those of the fifth column (by multiplying with appropriate factors), while for $\alpha > 60^{\circ}$ quantities of the fifth column be used to establish those of the fifth row.

For conical rings with larger periphery on top, α is greater than 90° and cos α is negative. In this case, we shall take the larger slant distance as s_i, the smaller slant distance as s_j ($\bar{r} < 1$), and we can use the same expression to obtain the flexibility matrix of the element, provided a change of sign is applied to the values thus obtained for all the third and fourth column quantities (f_{ij}, i = 1 to 5, j = 3,4) and to the last three of the fifth column quantities (f_{35}, f_{45}, f_{55}). This flexibility matrix after inversion will represent the stiffness of the conical ring.

2. Cylindrical Segment. For the cylindrical ring, the effects of the bending forces and the membrane force also should be treated separately. Both the bending solution and membrane solution for axi-symmetrical cylinders are available in Ref. (1) and (2). Using the notations and sign convention by Flügge[1] (Fig. 2), we established, after considerable amount of manipulation, the required relationships.

With a force N lbs. per inch applied at one end of cylinder, there must be an equal force N at the other end. The deformations due to membrane force N are

$$\begin{aligned} w &= -\frac{\nu\, Na}{Et} \\ e &= u_j - u_i = \frac{N(x_j - x_i)}{Et} \\ \frac{dw}{dx} &= 0 \end{aligned} \qquad \text{(IV-a)}$$

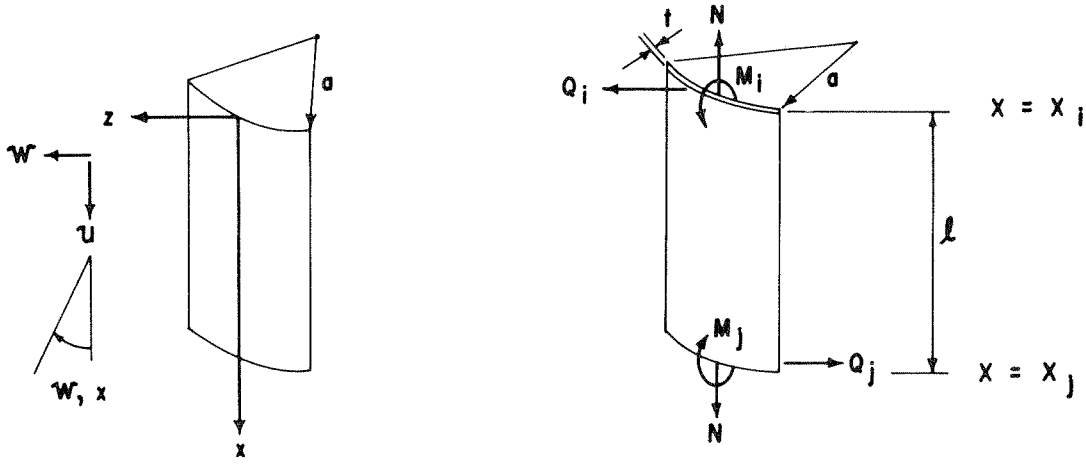

FIG. 2 - FORCES AND DEFORMATIONS IN A CYLINDRICAL ELEMENT

The bending solution of axi-symmetrical cylindrical sections yields

$$M_x = \frac{2K\kappa^2}{a^2}\left[e^{-\kappa\xi}(C_1 \sin\kappa\xi - C_2\cos\kappa\xi) - e^{\kappa\xi}(C_3\sin\kappa\xi - C_4\cos\kappa\xi)\right]$$

$$Q_x = \frac{2K\kappa^3}{a^3}\left\{e^{-\kappa\xi}\left[(C_1 + C_2)\cos\kappa\xi - (C_1 - C_2)\sin\kappa\xi\right] - e^{\kappa\xi}\left[(C_3 - C_4)\cos\kappa\xi + (C_3 + C_4)\sin\kappa\xi\right]\right\} \qquad \text{(IV-b)}$$

$$w = e^{-\kappa\xi}\left[C_1\cos\kappa\xi + C_2\sin\kappa\xi\right] + e^{\kappa\xi}\left[C_3\cos\kappa\xi + C_4\sin\kappa\xi\right]$$

$$\chi = \frac{dw}{dx} = \frac{1}{a}\frac{dw}{d\xi} = -\frac{\kappa}{a}e^{-\kappa\xi}\left[(C_1 - C_2)\cos\kappa\xi + (C_1 + C_2)\sin\kappa\xi\right] + \frac{\kappa}{a}e^{\kappa\xi}\left[(C_3 + C_4)\cos\kappa\xi - (C_3 - C_4)\sin\kappa\xi\right]$$

$$u = -\frac{\nu}{2\kappa}\left\{e^{-\kappa\xi}\left[(-C_1 - C_2)\cos\kappa\xi + (C_1 - C_2)\sin\kappa\xi\right] + e^{\kappa\xi}\left[(C_3 - C_4)\cos\kappa\xi + (C_3 + C_4)\sin\kappa\xi\right]\right\} + C$$

where $K = \dfrac{Et^3}{12(1-\nu^2)}$, $\kappa^4 = 3(1-\nu^2)\dfrac{a^2}{t^2}$, $\xi = \dfrac{x}{a}$

C_1 , C_2 , C_3 , C_4 , and C are constants of integration. The constants C_1 , C_2 , C_3 , C_4 can be determined by defining two force quantities at each end of the ring, and the constant C will drop out when only the expression of $e = u_j - u_i$ is wanted.

To conform to the particular force and deformation system adopted as standard for our process (see Fig. 1 and Eqs. (5)), we apply the four conditions

$$
\begin{aligned}
&\text{at } \xi = \xi_i = 0 && M_x = M_i \\
&\text{at } \xi = \xi_i = 0 && Q_x = -H_i \\
&\text{at } \xi = \xi_j = \frac{\ell}{a} && M_x = M_j \\
&\text{at } \xi = \xi_j = \frac{\ell}{a} && Q_x = -H_j
\end{aligned} \qquad (9)
$$

To obtain expressions of C_1, C_2, C_3, C_4 in terms of M_i, M_j, H_i, H_j.

Upon substitution of these expressions into (IV-b), there result (reference to Eq. (5)):

$$
\begin{aligned}
\bar{\chi}_i = \frac{K}{a} \Big\{ & (C_{11} - C_{21} - C_{31} - C_{41}) \cdot M_i + (C_{12} - C_{22} - C_{32} - C_{42}) \cdot M_j \\
& + (C_{13} - C_{23} - C_{33} - C_{43}) \cdot M_i + (C_{14} - C_{24} - C_{34} - C_{44}) \cdot H_j \Big\}
\end{aligned}
$$

$$
\begin{aligned}
\bar{\chi}_j = \frac{K}{a} \Big\{ & \Big[-e^{-\omega}(\cos\omega + \sin\omega)\, C_{11} + e^{-\omega}(\cos\omega - \sin\omega)\, C_{21} \\
& + e^{\omega}(\cos\omega - \sin\omega)\, C_{31} + e^{\omega}(\cos\omega + \sin\omega)\, C_{41} \Big] \cdot M_i \\
& + \Big[-e^{-\omega}(\cos\omega + \sin\omega)\, C_{12} + e^{-\omega}(\cos\omega - \sin\omega)\, C_{22} \\
& + e^{\omega}(\cos\omega - \sin\omega)\, C_{32} + e^{\omega}(\cos\omega + \sin\omega)\, C_{42} \Big] \cdot M_j \\
& + \Big[-e^{-\omega}(\cos\omega + \sin\omega)\, C_{13} + e^{-\omega}(\cos\omega - \sin\omega)\, C_{23} \\
& + e^{\omega}(\cos\omega - \sin\omega)\, C_{33} + e^{\omega}(\cos\omega + \sin\omega)\, C_{43} \Big] \cdot H_i \\
& + \Big[-e^{-\omega}(\cos\omega + \sin\omega)\, C_{14} + e^{-\omega}(\cos\omega - \sin\omega)\, C_{24} \\
& + e^{\omega}(\cos\omega - \sin\omega)\, C_{34} + e^{\omega}(\cos\omega + \sin\omega)\, C_{44} \Big] \cdot H_j \Big\}
\end{aligned}
$$

$$
\bar{\delta}_i = (-C_{11} - C_{31}) \cdot M_i + (-C_{12} - C_{32}) \cdot M_j + (-C_{13} - C_{33}) \cdot H_i + (-C_{14} - C_{34}) \cdot H_j
$$

$$
\begin{aligned}
\bar{\delta}_j = & (e^{-\omega}\cos\omega \cdot C_{11} + e^{-\omega}\sin\omega \cdot C_{21} + e^{\omega}\cos\omega \cdot C_{31} + e^{\omega}\sin\omega \cdot C_{41}) \cdot M_i \\
& + (e^{-\omega}\cos\omega \cdot C_{12} + e^{-\omega}\sin\omega \cdot C_{22} + e^{\omega}\cos\omega \cdot C_{32} + e^{\omega}\sin\omega \cdot C_{42}) \cdot M_j \\
& + (e^{-\omega}\cos\omega \cdot C_{13} + e^{-\omega}\sin\omega \cdot C_{23} + e^{\omega}\cos\omega \cdot C_{33} + e^{\omega}\sin\omega \cdot C_{43}) \cdot H_i \\
& + (e^{-\omega}\cos\omega \cdot C_{14} + e^{-\omega}\sin\omega \cdot C_{24} + e^{\omega}\cos\omega \cdot C_{34} + e^{\omega}\sin\omega \cdot C_{44}) \cdot H_j
\end{aligned}
$$

$$e = \frac{\nu}{2K}\left\{\left[e^{-\omega}(\cos\omega - \sin\omega)-1\right]\cdot C_{13} + \left[e^{-\omega}(\cos\omega + \sin\omega)-1\right]\cdot C_{23} - \left[e^{\omega}(\cos\omega + \sin\omega)-1\right]\cdot C_{33} + \left[e^{\omega}(\cos\omega - \sin\omega)-1\right]\cdot C_{43}\right\}\cdot H_i + \frac{\nu}{2K}\left\{\left[e^{-\omega}(\cos\omega - \sin\omega)-1\right]\cdot C_{14} + \left[e^{-\omega}(\cos\omega + \sin\omega)-1\right]\cdot C_{24} - \left[e^{\omega}(\cos\omega + \sin\omega)-1\right]\cdot C_{34} + \left[e^{\omega}(\cos\omega - \sin\omega)-1\right]\cdot C_{44}\right\}\cdot H_j$$

where $\omega = K\frac{\ell}{a}$, $C_{11}, C_{12} \ldots\ldots C_{43}, C_{44}$ satisfy the relations

$$\begin{aligned} C_1 &= C_{11}\cdot M_i + C_{12}\cdot M_j + C_{13}\cdot H_i + C_{14}\cdot H_j \\ C_2 &= C_{21}\cdot M_i + C_{22}\cdot M_j + C_{23}\cdot H_i + C_{24}\cdot H_j \\ C_3 &= C_{31}\cdot M_i + C_{32}\cdot M_j + C_{33}\cdot H_i + C_{34}\cdot H_j \\ C_4 &= C_{41}\cdot M_i + C_{42}\cdot M_j + C_{43}\cdot H_i + C_{44}\cdot H_j \end{aligned} \qquad (10)$$

$$C_{11} = \frac{D_{11}}{\Delta}\frac{a^2}{2KK^2}, \quad C_{12} = -\frac{D_{21}}{\Delta}\frac{a^2}{2KK^2}, \quad C_{13} = \frac{D_{31}}{\Delta}\frac{a^3}{2KK^3}, \quad C_{14} = -\frac{D_{41}}{\Delta}\frac{a^3}{2KK^3}$$

$$C_{21} = -\frac{D_{12}}{\Delta}\frac{a^2}{2KK^2}, \quad C_{22} = \frac{D_{22}}{\Delta}\frac{a^2}{2KK^2}, \quad C_{23} = -\frac{D_{32}}{\Delta}\frac{a^3}{2KK^3}, \quad C_{24} = \frac{D_{42}}{\Delta}\frac{a^3}{2KK^3}$$

$$C_{31} = \frac{D_{13}}{\Delta}\frac{a^2}{2KK^2}, \quad C_{32} = -\frac{D_{23}}{\Delta}\frac{a^2}{2KK^2}, \quad C_{33} = \frac{D_{33}}{\Delta}\frac{a^3}{2KK^3}, \quad C_{34} = -\frac{D_{43}}{\Delta}\frac{a^3}{2KK^3}$$

$$C_{41} = -\frac{D_{14}}{\Delta}\frac{a^2}{2KK^2}, \quad C_{42} = \frac{D_{24}}{\Delta}\frac{a^2}{2KK^2}, \quad C_{43} = -\frac{D_{34}}{\Delta}\frac{a^3}{2KK^3}, \quad C_{44} = \frac{D_{44}}{\Delta}\frac{a^3}{2KK^3}$$

$$\Delta = \left[2\sin\omega + (e^{\omega} - e^{-\omega})\right]\cdot\left[2\sin\omega - (e^{\omega} - e^{-\omega})\right]$$

$$D_{11} = \cos 2\omega - \sin 2\omega - e^{2\omega}$$

$$D_{21} = -(\cos\omega + \sin\omega)(e^{\omega} - e^{-\omega}) - 2\sin\omega\cdot e^{\omega}$$

$$D_{31} = e^{2\omega} - 1 - \sin 2\omega$$

$$D_{41} = \cos\omega\,(e^{\omega} - e^{-\omega}) - 2\sin\omega\cdot e^{\omega}$$

$$D_{12} = (\cos\omega - \sin\omega)^2 + 2\sin^2\omega - e^{2\omega}$$

$$D_{22} = -\cos\omega\,(e^{\omega} - e^{-\omega}) - \sin\omega\,(e^{\omega} + e^{-\omega})$$

$$D_{32} = 2\sin^2\omega$$

$$D_{42} = -\sin\omega\,(e^{\omega} - e^{-\omega})$$

$$D_{13} = -e^{-2\omega} + \sin 2\omega + \cos 2\omega$$

$$D_{23} = (\cos\omega - \sin\omega)(e^{\omega} - e^{-\omega}) + 2\sin\omega \cdot e^{-\omega}$$

$$D_{33} = 1 - e^{-2\omega} - \sin 2\omega$$

$$D_{43} = \cos\omega\,(e^{\omega} - e^{-\omega}) - 2\sin\omega \cdot e^{-\omega}$$

$$D_{14} = e^{-2\omega} - 2\sin^2\omega - \sin 2\omega - 1$$

$$D_{24} = -\cos\omega\,(e^{\omega} - e^{-\omega}) - \sin\omega(e^{\omega} + e^{-\omega})$$

$$D_{34} = 2\sin^2\omega$$

$$D_{44} = -\sin\omega\,(e^{\omega} - e^{-\omega})$$

Equations (IV-a) yield

$$\begin{aligned} \bar{\chi}_i &= 0 \\ \bar{\chi}_j &= 0 \\ \bar{\delta}_i &= -w_i = \frac{\nu a}{Et} N \\ \bar{\delta}_j &= w_j = -\frac{\nu a}{Et} N \\ e &= \frac{\ell}{Et} N \end{aligned} \qquad (11)$$

From Eqs. (10) and (11), the flexibility matrix of a cylindrical ring can be obtained such that

$$\begin{Bmatrix} \bar{\chi}_i \\ \bar{\chi}_j \\ \bar{\delta}_i \\ \bar{\delta}_j \\ e \end{Bmatrix} = \begin{bmatrix} f \end{bmatrix} \cdot \begin{Bmatrix} M_i \\ M_j \\ H_i \\ H_j \\ N \end{Bmatrix} \qquad (12)$$

in which f_{15} , f_{25} , f_{51} , f_{52} are known to be zeros. The stiffness of the cylindrical ring is obtained by inversion of the f matrix.

3. Spherical Cap. Flügge and Timoshenko both present the asymptotic solution for bending of shallow spherical shell in their books[1][2]. The resulting general expressions are given below with the notations shown in Fig. 3.

$$w = C_1 \text{ ber } x + C_2 \text{ bei } x + C_3 \text{ kei } x - C_4 \text{ ker } x + C_6$$

$$v = -\frac{\ell}{a}(1+\nu)\left\{ C_1 \text{ bei}'x - C_2 \text{ ber}'x - C_3 \text{ ker}'x - C_4 \text{ kei}'x - \frac{C_5}{x} + C_6 \frac{x}{(1+\nu)} \right\}$$

$$\chi = \frac{1}{\ell}(C_1 \text{ ber}'x + C_2 \text{ bei}'x + C_3 \text{ kei}'x - C_4 \text{ ker}'x)$$

$$M_r = \frac{K}{\ell^2}\left\{ C_1\left[-\text{bei } x - \frac{1}{x}(1-\nu)\text{ber}'x\right] + C_2\left[\text{ber } x - \frac{1}{x}(1-\nu)\text{bei}'x\right] + C_3\left[\text{ker } x - \frac{1}{x}(1-\nu)\text{kei}'x\right] - C_4\left[-\text{kei } x - \frac{1}{x}(1-\nu)\text{ker}'x\right]\right\}$$

$$M_\theta = \frac{K}{\ell^2}\left\{ C_1\left[(1-\nu)\frac{1}{x}\text{ber}'x - \nu \text{ bei } x\right] + C_2\left[(1-\nu)\frac{1}{x}\text{bei}'x + \nu \text{ ber } x\right] + C_3\left[(1-\nu)\frac{1}{x}\text{kei}'x + \nu \text{ ker } x\right] - C_4\left[(1-\nu)\frac{1}{x}\text{ker}'x - \nu \text{ kei } x\right]\right\} \qquad \text{(V-a)}$$

$$N_r = -\frac{Et}{a}\left[C_2 \cdot \frac{1}{x}\text{ber}'x - C_1 \frac{1}{x}\text{bei}'x + C_4 \frac{1}{x}\text{kei}'x + C_3 \frac{1}{x}\text{ker}'x + C_5 \frac{1}{x^2}\right]$$

$$N_\theta = -\frac{Et}{a}\left[C_2\left(-\text{bei } x - \frac{1}{x}\text{ber}'x\right) - C_1\left(\text{ber } x - \frac{1}{x}\text{bei}'x\right) + C_4\left(\text{ker } x - \frac{1}{x}\text{kei}'x\right) + C_3\left(-\text{kei } x - \frac{1}{x}\text{ker}'x\right) - \frac{C_5}{x^2}\right]$$

$$Q_r = \frac{K}{\ell^3}\left[-C_1 \text{ bei}'x + C_2 \text{ ber}'x + C_3 \text{ ker}'x + C_4 \text{ kei}'x\right]$$

From the above for shallow shells, the horizontal and vertical components of forces and displacements can be found with the relations:

$$
\begin{aligned}
H &= N_r - \frac{r}{a} Q_r \\
Q_v &= N_r \cdot \frac{r}{a} + Q_r \\
\delta_h &= v + \frac{r}{a} w \\
\delta_v &= \frac{r}{a} v - w
\end{aligned}
\qquad (13)
$$

The solution with six constants of integration is very general, and applies to both the cases with and without a singularity at the apex.

Using the second of Eq. (13), we find

$$Q_v = - \frac{Et\ell}{a^2} \frac{C_5}{x} \qquad (V\text{-}b)$$

Flügge mentions[1] that C_5 is related to the total vertical force applied above a horizontal section at which the forces are considered. Thus, C_5 is dependent on the manner in which the spherical shell is held in vertical equilibrium. We shall discuss the cases with and without singularity and their relation to our problem separately.

a) <u>The Case with Singularity</u>. Suppose the cap in Fig. 4 is supported by a concentrated force P at the apex. Then apparently C_5 is equal to a certain multiple of that force.

$$C_5 = -\frac{P}{2\pi}\frac{\ell^2}{K}$$

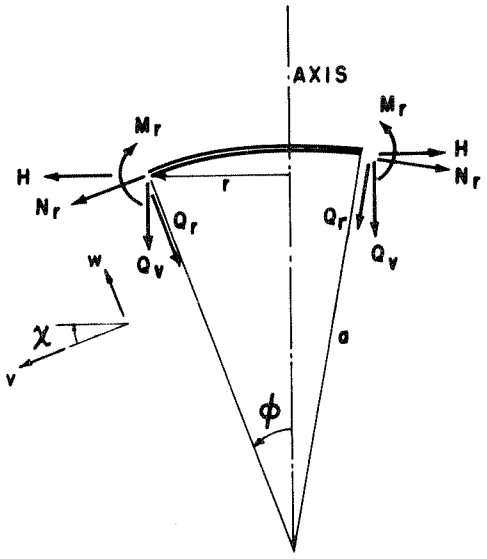

$$\ell = \frac{\sqrt{at}}{\sqrt[4]{12(1-\nu^2)}}$$

$$x = \frac{r}{\ell}$$

$$K = \frac{Et^3}{12(1-\nu^2)}$$

FIG. 3 - SHALLOW SPHERICAL CAP

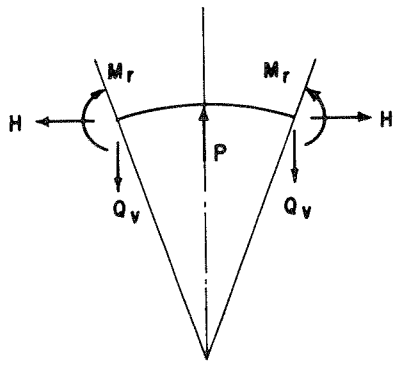

FIG. 4

Since the cap is under the combined action of P at the apex and Q_v around the periphery, the corresponding deformation must be the change of height of the cap. If we choose the apex of the cap as reference point, i.e., $(w)_{r=0} = 0$, then $(\delta_v)_{edge} = (\delta_v)_{edge} - (w)_{r=0}$ represents the increase in height of the cap. The horizontal deformation δ_h and change of slope χ offer no ambiguity. The conditions

at $r = x = 0$, w and χ must be finite

at $r = x = 0$, $w = 0$

at $r = x = 0$, N_r and N_θ must be finite[1]

result in $C_4 = C_6 = 0$, $C_3 = C_5$.

The remaining three constants C_1, C_2, C_5 can be determined by defining three quantities at the edge:

at $x = x_o$ $(r = r_o)$, $M_r = M_o$, $H = H_o$, $Q_v = Q_o$

Then the deformations of the edge can be expressed in the following forms.

$$\chi_o = \frac{1}{\ell}(C_{11}\,ber'x_o + C_{21}\,bei'x_o)M_o + \frac{1}{\ell}(C_{12}\,ber'x_o + C_{22}\,bei'x_o)H_o + \left(\frac{1}{\ell}C_{13}\,ber'x_o + \frac{1}{\ell}C_{23}\,bei'x_o - \frac{\ell\, r_o}{K}\,kei'x_o\right)Q_o$$

$$\begin{aligned}\delta h_o = {} & \frac{\ell}{a}\left\{C_{11}\left[x_o\,ber\,x_o - (1+\nu)\,bei'x_o\right] + C_{21}\left[x_o\,bei\,x_o + (1+\nu)\,ber'x_o\right]\right\}M_o \\ & + \frac{\ell}{a}\left\{C_{12}\left[x_o\,ber\,x_o - (1+\nu)\,bei'x_o\right] + C_{22}\left[x_o\,bei\,x_o + (1+\nu)\,ber'x_o\right]\right\}H_o \\ & + \left\{\frac{\ell}{a}C_{13}\left[x_o\,ber\,x_o - (1+\nu)\,bei'x_o\right] + \frac{\ell}{a}C_{23}\left[x_o\,bei\,x_o + (1+\nu)\,ber'x_o\right] - \frac{\ell^3 r_o}{a\,K}\left[x_o\,kei\,x_o + (1+\nu)\,ker'x_o + \frac{(1+\nu)}{x_o}\right]\right\}Q_o\end{aligned}$$

$$\delta v_o = \left\{ C_{11}\left[-\frac{\ell^2}{a^2} x_o (1+\nu)\, \mathrm{bei}'x_o - \mathrm{ber}\, x_o \right] + C_{21}\left[\frac{\ell^2 x_o}{a^2} (1+\nu)\, \mathrm{ber}'x_o - \mathrm{bei}\, x_o \right] \right\} M_o$$

$$+ \left\{ C_{12}\left[-\frac{\ell^2}{a^2} x_o (1+\nu)\, \mathrm{bei}'x_o - \mathrm{ber}\, x_o \right] + C_{22}\left[\frac{\ell^2 x_o}{a^2} (1+\nu)\, \mathrm{ber}'x_o - \mathrm{bei}\, x_o \right] \right\} H_o$$

$$+ \left\{ C_{13}\left[-\frac{\ell^2}{a^2} x_o (1+\nu)\, \mathrm{bei}'x_o - \mathrm{ber}\, x_o \right] + C_{23}\left[\frac{\ell^2 x_o}{a^2} (1+\nu)\, \mathrm{ber}'x_o - \mathrm{bei}\, x_o \right] - \frac{\ell^2 r_o}{K}\left[\frac{\ell^2 x_o}{a^2} (1+\nu)\left(\mathrm{ker}'x_o + \frac{1}{x_o}\right) - \mathrm{kei}\, x_o \right] \right\} Q_o$$

where

$$C_{11} = -\frac{1}{\Delta}\frac{\ell^2}{K}\, \mathrm{ber}'x_o \qquad \text{(VI-a)}$$

$$C_{12} = -\frac{1}{\Delta}\frac{a^3 x_o}{Et(a^2 + r_o^2)}\left[\mathrm{ber}\, x_o - \frac{(1-\nu)}{x_o}\, \mathrm{bei}'x_o \right]$$

$$C_{13} = \frac{1}{\Delta}\left\{ \left[\mathrm{ber}\, x_o \cdot \mathrm{ker}'x_o - \mathrm{ber}'x_o \cdot \mathrm{ker}\, x_o - \frac{(1-\nu)}{x_o}\, \mathrm{bei}'x_o \cdot \mathrm{ker}'x_o + \frac{(1-\nu)}{x_o}\, \mathrm{ber}'x_o \cdot \mathrm{ker}'x_o \right] \cdot \frac{\ell^2 r_o}{K} + \left[\mathrm{ber}\, x_o - \frac{(1-\nu)}{x_o}\, \mathrm{bei}'x_o \right] \cdot \frac{\ell^3 a^2}{K(a^2 + r_o^2)} \right\}$$

$$C_{21} = -\frac{1}{\Delta}\frac{\ell^2}{K}\, \mathrm{bei}'x_o$$

$$C_{22} = -\frac{1}{\Delta}\frac{a^3 x_o}{Et(a^2 + r_o^2)}\left[\mathrm{bei}\, x_o + \frac{(1-\nu)}{x_o}\, \mathrm{ber}'x_o \right]$$

$$C_{23} = \frac{1}{\Delta}\left\{\left[\text{bei } x_o \cdot \text{ker}'x_o - \text{bei}'x_o \cdot \text{ker } x_o + \frac{(1-\nu)}{x_o}\,\text{ber}'x_o \cdot \text{ker}'x_o + \frac{(1-\nu)}{x_o}\,\text{bei}'x_o \cdot \text{kei}'x_o\right] \cdot \frac{\ell^2 r_o}{K} + \left[\text{bei } x_o + \frac{(1-\nu)}{x_o}\,\text{ber}'x_o\right] \cdot \frac{\ell^3 a^2}{K(a^2 + r_o^2)}\right\}$$

and $$\Delta = \begin{vmatrix} -\left[\text{bei } x_o + \frac{(1-\nu)}{x_o}\,\text{ber}'x_o\right] & \left[\text{ber } x_o - \frac{(1-\nu)}{x_o}\,\text{bei}'x_o\right] \\ \text{bei}'x_o & -\text{ber}'x_o \end{vmatrix}$$

From Eq. (VI-a), the following relationship can be developed.

$$\begin{Bmatrix} \chi_o \\ \delta h_o \\ \delta v_o \end{Bmatrix} = \left[f_o\right] \cdot \begin{Bmatrix} M_o \\ H_o \\ Q_o \end{Bmatrix} \qquad (14)$$

or in matrix notation: $v_o = f_o \cdot S_o$

The 3x3 flexibility matrix f_o defined by (14) theoretically should be symmetrical. An actual example showed that there are slight discrepancies between terms on opposite sides of the main diagonal. This is due to the asymptotic nature of the solution and the use of 1 and r/a for cosine and sine of the extended angle ϕ_o. The use of this f matrix in an actual problem in general yielded satisfactory results except for a local "hump" near the singular support. However, such local phenomenon can be minimized if the size of the cap is made very small. In certain cases, such as the examples using approximate joint loads (see examples in Section IV), a 3x3 flexibility matrix like this one is essential for obtaining the correct answer.

b) The Case Without Singularity. When the vertical force Q_v is balanced by some distributed pressure instead of a single force P at apex, different constants of integration are required to achieve a solution. For finite deformations and finite membrane forces at the apex, C_3 and C_4 must vanish. If we again consider the apex as the vertical reference point, i.e, $w = 0$ at $r = x = 0$, then $C_6 = -C_1$. The remaining three constants C_1, C_2, C_5 are eliminated by defining three quantities M_o, H_o, Q_o at $x = x_o$ as before. On this basis, the expressions for edge deformations become:

$$\chi_o = -\frac{\ell}{\Delta K}\left[(\mathrm{ber}'x_o)^2 + (\mathrm{bei}'x_o)^2\right]\cdot M_o - \frac{a^3 x_o}{\Delta E t \ell (a^2 + r_o^2)}\cdot \left[\mathrm{bei}\, x_o \cdot \mathrm{bei}'x_o + \mathrm{ber}\, x_o \cdot \mathrm{ber}'x_o\right]\cdot H_o + \frac{a^4}{\Delta E t \ell^2 (a^2 + r_o^2)}\left[\mathrm{ber}\, x_o \cdot \mathrm{ber}'x_o + \mathrm{bei}\, x_o \cdot \mathrm{bei}'x_o\right]\cdot Q_o$$

$$\delta h_o = -\frac{\ell^3 x_o}{a K \cdot \Delta}\left\{\mathrm{ber}\, x_o \cdot \mathrm{ber}'x_o + \mathrm{bei}\, x_o \cdot \mathrm{bei}'x_o\right\}\cdot M_o - \frac{\ell a^2}{\Delta \cdot E t (a^2 + r_o^2)}\left\{x_o^2\left[(\mathrm{ber}\, x_o)^2 + (\mathrm{bei}\, x_o)^2\right] + 2 x_o\left[\mathrm{bei}\, x_o \cdot \mathrm{ber}'x_o - \mathrm{ber}\, x_o \cdot \mathrm{bei}'x_o\right] + (1 - \nu^2)\left[(\mathrm{ber}'x_o)^2 + (\mathrm{bei}'x_o)^2\right]\right\}\cdot H_o + \frac{a^3}{\Delta \cdot E t (a^2 + r_o^2)}\left\{x_o\left[(\mathrm{ber}\, x_o)^2 + (\mathrm{bei}\, x_o)^2\right] + 2\left[\mathrm{bei}\, x_o \cdot \mathrm{ber}'x_o - \mathrm{ber}\, x_o \cdot \mathrm{bei}'x_o\right] + \frac{(1-\nu^2)}{x_o}\left[(\mathrm{ber}'x_o)^2 + (\mathrm{bei}'x_o)^2\right]\right\}\cdot Q_o - (1 + \nu)\frac{a}{Et} Q_o \qquad \text{(VI-b)}$$

$$\delta v_o = \frac{\ell^2}{\Delta K}\left\{ \text{ber } x_o \cdot \text{ber}'x_o + \text{bei } x_o \cdot \text{bei}'x_o - \left(\frac{x_o^2 \ell^2}{a^2} + 1\right) \text{ber}'x_o \right\} \cdot M_o$$

$$+ \frac{a^3 x_o}{\Delta\, Et(a^2 + r_o^2)} \left\{ \left[(\text{ber } x_o)^2 + (\text{bei } x_o)^2 \right] \right.$$

$$+ \left[\frac{x_o \ell^2}{a^2}(1+\nu) - \frac{(1-\nu)}{x_o} \right] \cdot \left[\text{ber } x_o \cdot \text{bei}'x_o - \text{bei } x_o \cdot \text{ber}'x_o \right]$$

$$- \frac{\ell^2}{a^2}(1-\nu^2) \left[(\text{ber}'x_o)^2 + (\text{bei}'x_o)^2 \right]$$

$$\left. - \left(\frac{x_o^2 \ell^2}{a^2} + 1\right) \left[\text{ber } x_o - \frac{(1-\nu)}{x_o} \text{bei}'x_o \right] \right\} \cdot H_o$$

$$+ \frac{a^4}{\Delta\, Et \cdot \ell (a^2 + r_o^2)} \left\{ - \left[(\text{ber } x_o)^2 + (\text{bei } x_o)^2 \right] \right.$$

$$- \left[\frac{x_o \ell^2}{a^2}(1+\nu) - \frac{(1-\nu)}{x_o} \right] \cdot \left[\text{ber } x_o \cdot \text{bei}'x_o - \text{bei } x_o \cdot \text{ber}'x_o \right]$$

$$+ \frac{\ell^2}{a^2}(1-\nu^2) \left[(\text{ber}'x_o)^2 + (\text{bei}'x_o)^2 \right]$$

$$\left. + \left(\frac{x_o^2 \ell^2}{a^2} + 1\right) \left[\text{ber } x_o - \frac{(1-\nu)}{x_o} \text{bei}'x_o \right] \right\} \cdot Q_o - \frac{(1+\nu) x_o \ell}{Et} Q_o$$

If we form a 3x3 flexibility matrix f_o from (VI-b) so as to satisfy (14), we find that the third column and the third row are not symmetrical with respect to the main diagonal. In this case Betti's law is not satisfied because the part of work done by the distributed pressure in vertical direction is not included by considering only the quantities appearing in Eq. (VI-b). Such a flexibility matrix cannot be used.

However, the relationships expressed by (VI-b) are valid, and the first 2x2 matrix obtained from (VI-b) is the same as that obtained from

(VI-a). This means that the force-deformation relationships in the horizontal and rotational senses are independent of the manner in which the cap is supported vertically. In our solution process using the exact joint loads (see Sections III,C,2 and IV,A), we shall make use of such a 2x2 flexibility matrix along with the first two coefficients of the last equation of (VI-b).

C. Joint Loads

In the finite element analysis, only the forces and displacements of certain discrete points of the structure are considered. These points are called the nodal points of the structure which are the junctions of the individual elements. For axi-symmetric shells of revolution, these nodal points are circles. If the structure is subjected to concentrated forces applied at the nodal points, the results of the analysis will be exact if the geometry of the element is exact. If distributed load exists, we can either consider the distributed load as concentrated at several nodal points, thus obtaining an approximate solution, or we can hold the nodal points fixed in space and determine the fixed-edge forces of each element. The reactions of these fixed-edge forces can be applied at the nodal points as concentrated joint loads. The element forces and deformations due to these concentrated joint loads superimposed on the fixed-edge forces and deformations yield the final answers. Next, we shall discuss the two alternative procedures in more details.

1. Approximate Joint Loads.

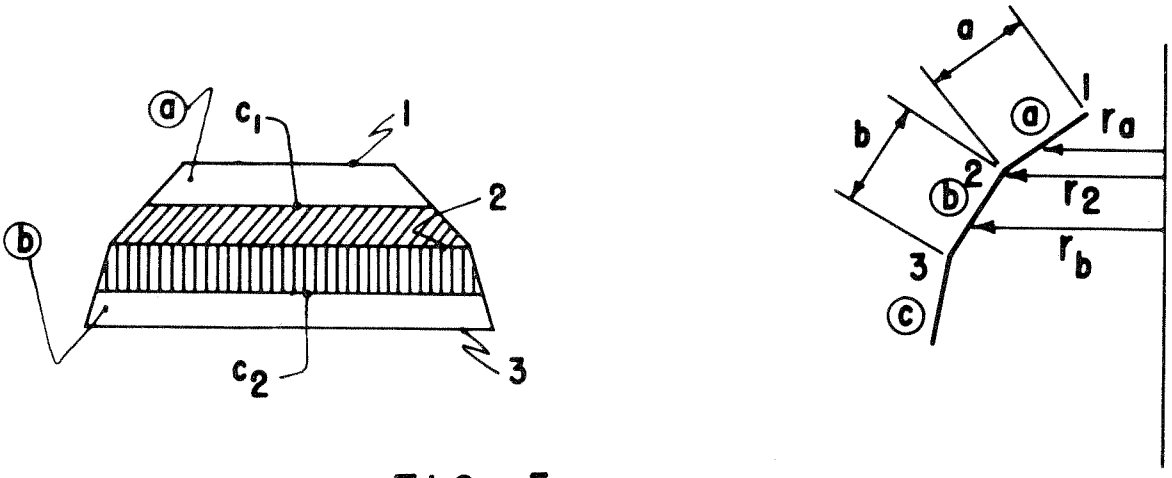

FIG. 5

Fig. 5 shows the developed surfaces of conical elements (a) and (b) with joints 1, 2, and 3; C_1 and C_2 are their respective centroids. The approximate load on joint 2 is due to the components of the total pressure on the shaded area. Thus, we developed an expression for the joint loads due to internal pressure p_r.

$$
\begin{aligned}
T_2 &= 0 \\
P_{h2} &= \left[\left(\frac{r_a + r_2}{2r_2} \right) a \sin \alpha_a + \left(\frac{r_2 + r_b}{2r_2} \right) b \sin \alpha_b \right] p_r \\
P_{v2} &= \left[\left(\frac{r_a + r_2}{2r_2} \right) a \cos \alpha_a + \left(\frac{r_2 + r_b}{2r_2} \right) b \cos \alpha_b \right] p_r
\end{aligned}
\qquad (15)
$$

where T_2, P_{h2}, P_{v2} are the moment, horizontal and vertical forces applied at joint 2, a and b are the meridianal lengths of the elements (a) and (b),

r_a, r_b are the horizontal radii of the centroidal circle of elements (a) and (b)

r_2 = horizontal radius of joint 2

α_a , α_b are the inclinations of elements (a) and (b) as defined in Fig. 1.

The loads contributed by pressure on the spherical cap are assumed entirely concentrated on the bottom edge of the cap.

Such approximations yield only vertical and horizontal forces and no moment for the joint loads. Actual calculations showed that the concentrated forces induce high negative moments at intermediate joints, even far from end restraints, where the action is known to be predominantly membrane.

As the sizes of the elements are made smaller, these negative joint moments decrease as to be expected. But in order to reduce these moments to the magnitudes of what they should be in a nearly membrane state of stress, we must divide the actual shell into a very large number of elements.

A solution using these approximate joint loads, which are considered as equivalent system to the actual loading, is quite satisfactory for the solution of problems. In this solution, it is necessary to use a 3x3 flexibility for the spherical cap (as discussed in III, B, 3-a). Otherwise, the results would show zero vertical element force in the cap which is not correct.

2. Joint Loads from Fixed-Edge Forces of the Element. A solution using this type of joint loads consists of the following steps: (Fig. 6)

(1) Fix all joints in space and compute the fixed-edge forces in all elements.

(2) Reverse these fixed-edge forces, apply them on the joints, and let the structure deform. Compute joint displacements. Then determine the forces and deformations in the elements.

(3) The final states of forces and deformations in the elements are obtained by adding (1) to (2).

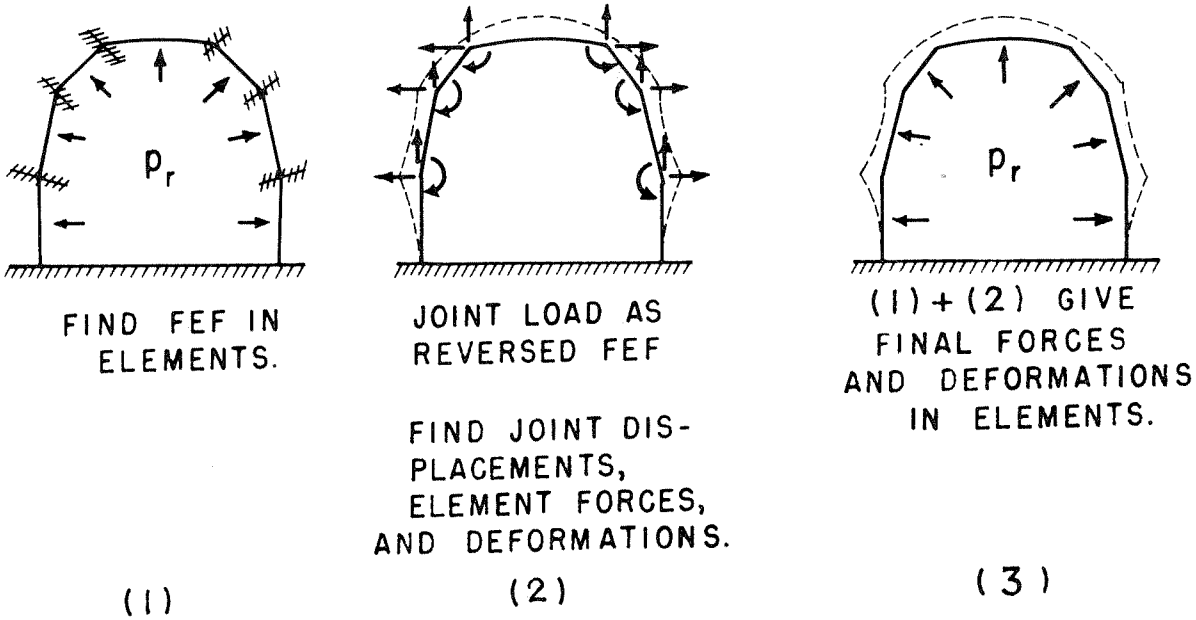

FIG. 6

For the case of ordinary structural frames the solution is exact. For the case of a shell, this solution, although exact in concept, does not yield more accurate results than that found using approximate joint loads. Moreover, this procedure involves more steps than the solution using approximate joint loads. Therefore, it was not found to be particularly advantageous. This will be discussed later in Section V.

The calculation of the fixed-edge forces in the spherical and conical elements needs some further comments.

a) Spherical Cap. Membrane solution of shallow spherical shell gives

$$\chi_{mo} = \frac{(1-\nu)}{2\,Et}\, p_r \cdot r_o$$

$$\delta h_{mo} = \frac{(1-\nu)}{2\,Et}\, p_r \cdot r_o \cdot a \qquad (16)$$

$$\delta v_{mo} = \frac{(1-\nu)}{2\,Et}\, p_r \cdot r_o^2$$

Eq. (16) gives the membrane deformations $\left\{ v_{mo} \right\}$ which have been defined in Fig. 3. (Subscript m indicates membrane action). The application of a set of edge forces $\left\{ S_{F_o} \right\}$ will produce edge deformations $\left\{ v_{F_o} \right\}$ which when added to $\left\{ v_m \right\}$ result in zero deformations. Thus,

$$v_{m_o} + v_{F_o} = 0$$

Since $v_{F_o} = f_o \cdot S_{F_o}$

$$f_o \cdot S_{F_o} = -v_{m_o} \qquad (17)$$

$$S_{F_o} = -f_o^{-1} \cdot v_{m_o}$$

For the case without singularity at apex, we use a 2x2 f_o matrix (refer to III, B, 3). Hence

$$\begin{Bmatrix} M_F \\ H_F \end{Bmatrix} = -\left[k_o \right] \cdot \begin{Bmatrix} \chi_{mo} \\ \delta h_{mo} \end{Bmatrix} \qquad (17a)$$

The third component of the element forces can be found separately:

$$Q_{vF} = \tfrac{1}{2}\, p_r \cdot a \cdot \sin \phi_o \qquad (18)$$

Fig. 7 shows the relations between the fixed edge forces of the cap and the joint forces, from which it is apparent that

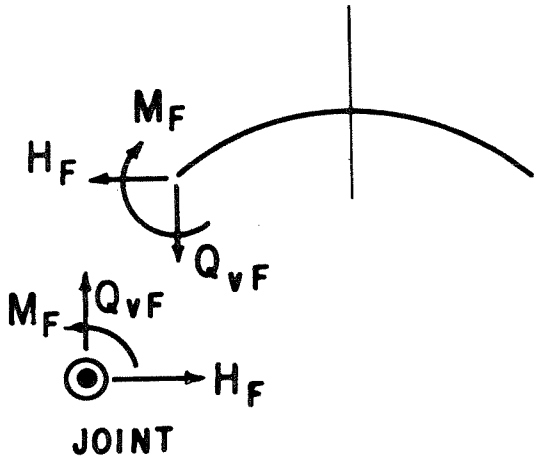

$$T = -M_F$$
$$P_h = -H_F$$
$$P_v = Q_{vF} \qquad (19)$$

or

$$\{R\} = \begin{bmatrix} -1 & 0 & 0 \\ 0 & -1 & 0 \\ 0 & 0 & 1 \end{bmatrix} \cdot \{S_F\}$$

FIG. 7

The 3x3 matrix in (19) is the equilibrium matrix of the spherical cap A_o (see III, D, 1) with a minus sign. Hence

$$R = -A_o \cdot S_F \qquad (20)$$

b) Conical Ring.

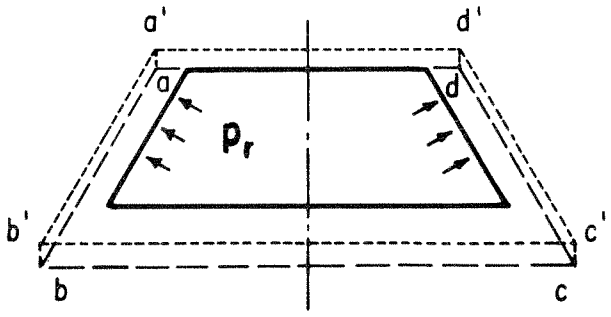

FIG. 8

Fig. 8 shows a conical ring under internal pressure p_r. To find the membrane displacements, we need some arbitrary support to balance the pressure vertically. For this purpose we choose to hold the cone at upper edge such that the meridianal displacement v of the top edge is zero. This, we recall, is the same boundary condition as used in determining the meridianal stretch in the flexibility matrix (see III, B, 1).

Under this assumption the displaced cone will be in the dotted position a'b'c'd'. (Note that angle changes are not shown in Fig. 8.) A rigid body displacement will bring the cone to the dashed position a b c d where the top edge of the cone is at the original level. We see that such a movement does not change the magnitudes of the horizontal displacements δ_{mi} and δ_{mj} and the meridianal stretch e_m. Thus the stiffness matrix obtained in III, B, 1 can be used directly to find the fixed-edge forces.

Membrane solution of conical shells gives:

$$N_{mi} = \frac{p_r \cot \alpha}{2} \left(s_i - \frac{s_j^2}{s_i}\right)$$

$$\bar{\chi}_{mi} = -\frac{p_r \cot^2 \alpha}{2\,Et} \left(3\,s_i + \frac{s_j^2}{s_i}\right)$$

$$\bar{\chi}_{mj} = \frac{p_r \cot^2 \alpha}{Et} \cdot 2\,s_j \qquad (21)$$

$$\bar{\delta}_{mi} = -\frac{p_r \cot^2 \alpha}{2\,Et \sin \alpha}\left[(2-\nu)s_i^2 + \nu\, s_j^2\right]$$

$$\bar{\delta}_{mj} = \frac{p_r \cos^2 \alpha}{Et \sin \alpha} \cdot s_j^2$$

$$e_m = \frac{p_r \cot \alpha}{4\,Et}\left[(1-2\nu)(s_j^2 - s_i^2) - 2\, s_j^2 \cdot \log \frac{s_j}{s_i}\right]$$

By the same reasoning as followed in (a)

$$S_F = -f^{-1} v_m = -k\, v_m \tag{22}$$

where $v_m = \begin{Bmatrix} \bar{\chi}_{mi} \\ \bar{\chi}_{mj} \\ \bar{\delta}_{mi} \\ \bar{\delta}_{mj} \\ e_m \end{Bmatrix}$ and $S_F = \begin{Bmatrix} M_{Fi} \\ M_{Fj} \\ H_{Fi} \\ H_{Fj} \\ N_{Fj} \end{Bmatrix}$

Also

$$R = -A\, S_F = A\, k\, v_m \tag{23}$$

or for the n^{th} element in general

$$R^{(n)} = \begin{Bmatrix} R_i^{(n)} \\ \\ R_j^{(n)} \end{Bmatrix} = A_n\, k^{(n)}\, v_m^{(n)} \tag{23-a}$$

where A_n is the equilibrium matrix relating the edge forces to the joint forces of the n^{th} element (see III, D, 1).

c) Cylindrical Ring. Equations (22) and (23) still hold except the stiffness and equilibrium matrices used should be those of the cylindrical element. The membrane deformations $\{v_m\}$ in this case are

$$\begin{aligned} \bar{\chi}_{mi} &= 0 \\ \bar{\chi}_{mj} &= 0 \\ \bar{\delta}_{mi} &= -\frac{p_r a^2}{Et} \\ \bar{\delta}_{mj} &= \frac{p_r a^2}{Et} \\ e_m &= -\frac{\nu\, p_r \cdot a \cdot \ell}{Et} \end{aligned} \tag{24}$$

With the joint loads determined in the above described manner, a standard matrix solution will yield

$$\bar{S}^{(n)} = \begin{Bmatrix} \bar{M}_i^{(n)} \\ \bar{M}_j^{(n)} \\ \bar{H}_i^{(n)} \\ \bar{H}_j^{(n)} \\ \bar{N}_j^{(n)} \end{Bmatrix}$$

which represent only the effect of the system of joint loads resulting from the unbalanced fixed-edge forces. The final edge forces in the n^{th} element are

$$S^{(n)} = \bar{S}^{(n)} + S_F^{(n)} \tag{25}$$

while $N_i^{(n)} = \bar{r}^{(n)} N_j^{(n)} + N_{mi}^{(n)}$.

D. Matrix Solution of the Problem

1. The Standard Matrix Operations. It was mentioned at the beginning of this section that four kinds of matrices are needed to solve a problem of axi-symmetrical shells of revolution. We have already discussed the formulation and application of the stiffness and load matrices. Now we shall show the formulation of the displacement transformation and equilibrium matrices.

Fig. 9 shows the positive directions of the loads and displacements of the nodal points or joints of the structure which are adopted in this report.

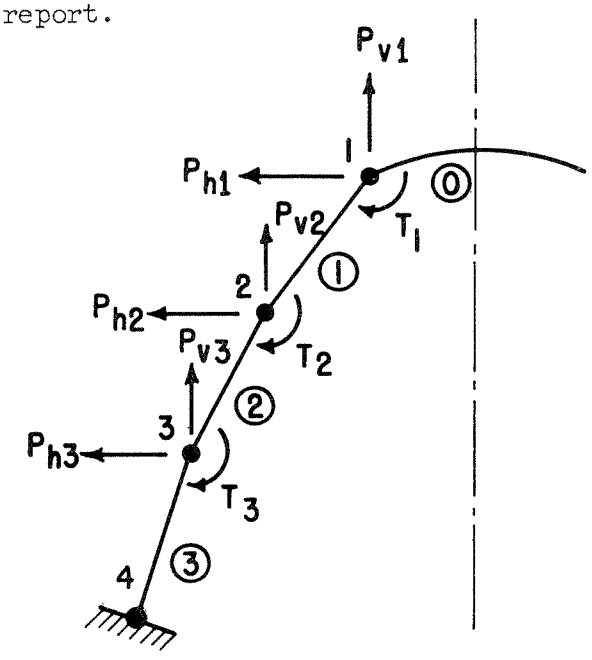

Joint displacements:

Θ - in direction of T, positive when flattens the element.

Δ_h - in direction of P_h, positive outward.

Δ_v - in direction of P_v, positive upward.

ELEMENTS = ⓪, ①, ②, ... ⓝ
JOINTS = 1, 2, 3, ... n+1

FIG. 9 - JOINT FORCES AND DISPLACEMENTS.

Remembering the definitions of the element forces and deformations (Figs. 1 and 2) we obtain the following relations:

$$\begin{cases} \chi_o = \theta_1 \\ \delta h_o = \Delta_{h1} \\ \delta v_o = -\Delta_{v1} \end{cases}$$

$$\begin{cases} \bar{\chi}_i^{(1)} = -\theta_1 \\ \bar{\chi}_j^{(1)} = +\theta_2 \\ \bar{\delta}_i^{(1)} = -\Delta_{h1} \\ \bar{\delta}_j^{(1)} = +\Delta_{h2} \\ e^{(1)} = -\cos\alpha_1 \cdot \Delta_{h1} + \sin\alpha_1 \cdot \Delta_{v1} + \cos\alpha_1 \Delta_{h2} - \sin\alpha_1 \cdot \Delta_{v2} \end{cases}$$

$$\begin{cases} \bar{\chi}_i^{(n)} = -\theta_n \\ \bar{\chi}_j^{(n)} = +\theta_{n+1} \\ \bar{\delta}_i^{(n)} = -\Delta_{hn} \\ \bar{\delta}_j^{(n)} = +\Delta_{hn+1} \\ e^{(n)} = -\cos\alpha_n \cdot \Delta_{hn} + \sin\alpha_n \Delta_{vn} + \cos\alpha_n \cdot \Delta_{hn+1} - \sin\alpha_n \cdot \Delta_{vn+1} \end{cases}$$

In matrix form:

$$\begin{Bmatrix} \chi_o \\ \delta h_o \\ \delta v_o \\ \bar{\chi}_i^{(1)} \\ \bar{\chi}_j^{(1)} \\ \vdots \\ \bar{\delta}_i^{(n)} \\ \bar{\delta}_j^{(n)} \\ e^{(n)} \end{Bmatrix} = \begin{bmatrix} 1 & 0 & 0 & & & & & \\ 0 & 1 & 0 & & & & & \\ 0 & 0 & -1 & & & & & \\ -1 & 0 & 0 & 0 & & & & \\ 0 & 0 & 0 & 1 & & & & \\ & & & & & & & \\ & & & & & & & \\ & & & & -1 & 0 & 0 & 0 & 0 \\ & & & & 0 & 0 & 0 & 1 & 0 \\ & & & & -\cos\alpha_n & \sin\alpha_n & 0 & \cos\alpha_n & -\sin\alpha_n \end{bmatrix} \begin{Bmatrix} \theta_1 \\ \Delta_{h1} \\ \Delta_{v1} \\ \theta_2 \\ \Delta_{h2} \\ \Delta_{v2} \\ \vdots \\ \theta_n \\ \Delta_{hn} \\ \Delta_{vn} \\ \theta_{n+1} \\ \Delta_{hn+1} \\ \Delta_{vn+1} \end{Bmatrix}$$

or

$$\begin{Bmatrix} v^{(0)} \\ v^{(1)} \\ v^{(2)} \\ \vdots \\ v^{(n)} \end{Bmatrix} = \begin{bmatrix} B_0\ 3\times3 & & & \\ & B_1\ 5\times6 & & \\ & & B_2\ 5\times6 & \\ & & & B_n\ 5\times6 \end{bmatrix} \cdot \begin{Bmatrix} r_1 \\ r_2 \\ r_3 \\ \vdots \\ r_{n+1} \end{Bmatrix}$$

Using symbolic notations:

$$v = B\,r \tag{26}$$

where v is the matrix representing edge deformations of all elements

r is the matrix representing the displacements of all joints

and B is the displacement transformation matrix.

Next, considering the equilibrium of each joint, with proper attention to the positive directions of the joint forces and element forces as defined in Fig. 1,2, and 9, we have

$$\begin{cases} T_1 = M_o - M_i^{(1)} \\ P_{h1} = H_o - H_i^{(1)} - \bar{r}^{(1)} \cos\alpha_1 \, N_j^{(1)} \\ P_{v1} = -Qv_o + \bar{r}^{(1)} \sin\alpha_1 \cdot N_j^{(1)} \end{cases}$$

$$\begin{cases} T_2 = M_j^{(1)} - M_i^{(2)} \\ P_{h2} = H_j^{(1)} - H_i^{(2)} + \cos\alpha_1 \cdot N_j^{(1)} - \bar{r}^{(2)} \cos\alpha_2 \, N_j^{(2)} \\ P_{v2} = -\sin\alpha_1 \cdot N_j^{(1)} + \bar{r}^{(2)} \sin\alpha_2 \cdot N_j^{(2)} \end{cases}$$

$$\begin{cases} T_n = M_j^{(n-1)} - M_i^{(n)} \\ P_{hn} = H_j^{(n-1)} - H_i^{(n)} + \cos\alpha_{n-1} \cdot N_j^{(n-1)} - \bar{r}^{(n)} \cos\alpha_n \cdot N_j^{(n)} \\ P_{vn} = -\sin\alpha_{n-1} \cdot N_j^{(n-1)} + \bar{r}^{(n)} \sin\alpha_n \cdot N_j^{(n)} \end{cases}$$

$$\begin{cases} T_{n+1} = M_j^{(n)} \\ P_{hn+1} = H_j^{(n)} + \cos\alpha_n \cdot N_j^{(n)} \\ P_{vn+1} = -\sin\alpha_n \cdot N_j^{(n)} \end{cases}$$

Note: for cylindrical element, $\alpha = 90^\circ$ $\sin\alpha = 1$, $\cos\alpha = 0$, $\bar{r} = 1$, the above relations still hold.

From these relations we can form

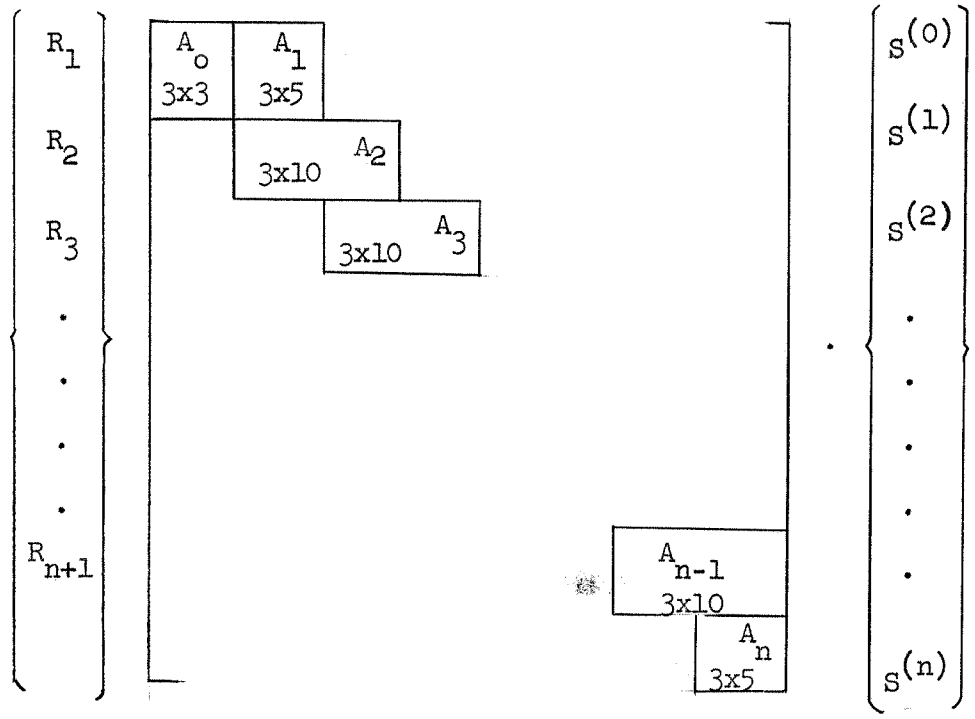

or using symbolic notations:

$$R = A\,S \tag{27}$$

where R is the matrix representing forces on all joints

S is the matrix representing edge forces of all elements

and A is the equilibrium matrix.

With v and S as defined in Eqs. (26) and (27), we can write

$$S = k\,v \tag{28}$$

where

$$k = \begin{bmatrix} k^{(0)} & & & & \\ & k^{(1)} & & & \\ & & k^{(2)} & & \\ & & & \ddots & \\ & & & & k^{(n)} \end{bmatrix}$$

and $k^{(0)} = f_o^{-1}$, $k^{(1)} = f_1^{-1}$, ... $k^{(n)} = f_n^{-1}$,

f_o is the flexibility matrix of the cap

f_1 ..... f_n are the flexibility matrices of the 1^{st}..... n^{th} cone or cylinder.

Eqs. (27), (28), (26) yield

$$R = A\,k\,B\,r = K\,r$$
$$K = A\,k\,B \qquad (29)$$

which relates directly the joint displacements r to the joint force R of the structure. The quantity K is called the stiffness of the structure.

With a given set of joint loads R we can find in sequence: r from (29), v from (26) and S from (28).

This process of solution, however, involves the operations with large matrices, such as A, B, k, consisting mostly of zeros and therefore, poses a problem of storage for the computer. Indeed, IBM 7090 can handle problems using only about 15 elements when this process is employed.

One way to avoid such a storage problem is to form the structural stiffness K directly by operating with small matrices A_n , B_n and $k^{(n)}$ instead of the large matrices A, B, and k. This process will be discussed in the next article.

2. The Direct Stiffness Method. To avoid the difficulty of having inadequate storage locations in the computer, we operate with the small submatrices A_n, B_n of the large matrices A and B appearing in Eqs. (27) and (26) together with the element stiffness $k^{(n)}$ and form the structural stiffness K in a different way.

In the previous article we have established for the first conical element the following relations:

$$\begin{aligned} S^{(1)} &= k^{(1)} \quad v^{(1)} \\ v^{(1)} &= B_1 \quad r_E(1) \\ R_E^{(1)} &= A_1 \quad S^{(1)} \end{aligned} \tag{30}$$

where $$R_E^{(1)} = \begin{Bmatrix} R_i^{(1)} \\ R_j^{(1)} \end{Bmatrix} = \begin{Bmatrix} T_i \\ P_{hi} \\ P_{vi} \\ T_j \\ P_{hj} \\ P_{vj} \end{Bmatrix}^{(1)} \qquad r_E^{(1)} = \begin{Bmatrix} r_i^{(1)} \\ r_j^{(1)} \end{Bmatrix} = \begin{Bmatrix} \theta_i \\ \Delta_{hi} \\ \Delta_{vi} \\ \theta_j \\ \Delta_{hj} \\ \Delta_{vj} \end{Bmatrix}^{(1)}$$

are the joint forces and joint displacements of the structure consisting of only one element, i.e., element (1).

Thus, the stiffness of the structure consisting of only element (1) is

$$K^{(1)} = A_1 \, k^{(1)} \, B_1$$

and similarly for the n^{th} structure, that is, the structure consisting of the n^{th} cone (or cylinder), only

$$K^{(n)} = A_n \, k^{(n)} \, B_n \tag{31}$$

For the spherical cap

$$K^{(0)} = A_o \; k^{(0)} \; B_o$$

and

$$R_E^{(0)} = K^{(0)} \; r_E^{(0)}$$

where $R_E^{(0)} = R_j^{(0)}$, $r_E^{(0)} = r_j^{(0)}$, since the cap has only a lower edge.

By partitioning of matrices, Eq. (31) can be rewritten as

$$R_E^{(n)} = \begin{Bmatrix} R_i^{(n)} \\ R_j^{(n)} \end{Bmatrix} = \left[\begin{array}{c|c} \bar{k}_{ii}^{(n)} & \bar{k}_{ij}^{(n)} \\ \hline \bar{k}_{ji}^{(n)} & \bar{k}_{jj}^{(n)} \end{array}\right] \cdot \begin{Bmatrix} r_i^{(n)} \\ r_j^{(n)} \end{Bmatrix}$$

where

$$\begin{aligned} \bar{k}_{ii}^{(n)} &= A_{ni} \cdot k^{(n)} \cdot B_{ni} \\ \bar{k}_{ij}^{(n)} &= A_{ni} \cdot k^{(n)} \cdot B_{nj} \\ \bar{k}_{ji}^{(n)} &= A_{nj} \cdot k^{(n)} \cdot B_{ni} \\ \bar{k}_{jj}^{(n)} &= A_{nj} \cdot k^{(n)} \cdot B_{nj} \end{aligned} \tag{32}$$

and A_{ni}, A_{nj}, B_{ni}, B_{nj} are submatrices of A_n and B_n such that

$$\left[A_n\right] = \left[\begin{array}{c} A_{ni} \\ \hline A_{nj} \end{array}\right], \qquad \left[B_n\right] = \left[\begin{array}{c|c} B_{ni} & B_{nj} \end{array}\right] .$$

Next, we note that the joint force at any joint in the assemblage is the sum of the forces on joints i and j of the lower and upper elements respectively, and the joint displacement of any joint in the assemblage is common for joints i and j of the lower and upper elements.

This means that

$$\begin{aligned} R_1 &= R_i^{(1)} + R_j^{(0)} & r_1 &= r_i^{(1)} = r_j^{(0)} \\ R_2 &= R_j^{(1)} + R_i^{(2)} & r_2 &= r_j^{(1)} = r_i^{(2)} \\ &\text{---------- and ----------} \\ R_n &= R_j^{(n-1)} + R_i^{(n)} & r_n &= r_j^{(n-1)} + r_i^{(n)} \\ R_{n+1} &= R_j^{(n)} & r_{n+1} &= r_j^{(n)} \end{aligned} \tag{33}$$

Using Equations (32) and (33), the structural stiffness of the assemblage may now be put into a tri-diagonal matrix form

$$\begin{Bmatrix} R_1 \\ R_2 \\ R_3 \\ \cdot \\ \cdot \\ R_{n+1} \end{Bmatrix} = \begin{bmatrix} (\bar{k}^{(0)}_{ii}+\bar{k}^{(1)}_{ii}) & \bar{k}^{(1)}_{ij} & \cdot & \cdot & \cdot \\ \bar{k}^{(1)}_{ji} & (\bar{k}^{(1)}_{jj}+\bar{k}^{(2)}_{ii}) & \bar{k}^{(2)}_{ij} & \cdot & \cdot \\ \cdot & \bar{k}^{(2)}_{ji} & (\bar{k}^{(2)}_{jj}+\bar{k}^{(3)}_{ii}) & \cdot & \cdot \\ \cdot & \cdot & \cdot & \cdot & \cdot \\ \cdot & \cdot & \cdot & (\bar{k}^{(n-1)}_{jj}+\bar{k}^{(n)}_{ii}) & \bar{k}^{(n)}_{ij} \\ \cdot & \cdot & \cdot & \bar{k}^{(n)}_{ji} & \bar{k}^{(n)}_{jj} \end{bmatrix} \cdot \begin{Bmatrix} r_1 \\ r_2 \\ r_3 \\ \cdot \\ \cdot \\ r_{n+1} \end{Bmatrix} \tag{34}$$

which is an expanded form of the relation

$$R = K \cdot r$$

and it should be noted that K as developed in Eq. (29) also can be stated in this form.

The process described in this article has the advantage that $\bar{k}_{ii}$, $\bar{k}_{ij}$, $\bar{k}_{ji}$, $\bar{k}_{jj}$ for each element are developed in a do-loop of the computer program, eliminating the storage of the large matrices A, B, and k. The final K matrix is the only large matrix which remains for subsequent calculations. If this K matrix is stored in a conventional rectangular form, the 7090 computer can handle problems involving 45 conical elements. By the use of subroutines of skew storage and solution* or by applying a recursion process[21] problems involving several hundred or more elements can be analyzed.

---

*Private communication from Messrs. A. De Fries and Ashvin Shah, Graduate students of University of California, Berkeley.

3. Special Methods for Shells Subject to Internal Pressure.

For shells subject to internal pressure only in which the stress conditions are essentially membrane except in regions near the restraints, some short-cut procedures can be used instead of the more general approaches discussed above. Two of such methods are described below.

a) Substitution of a known element force in place of a part of the structure.

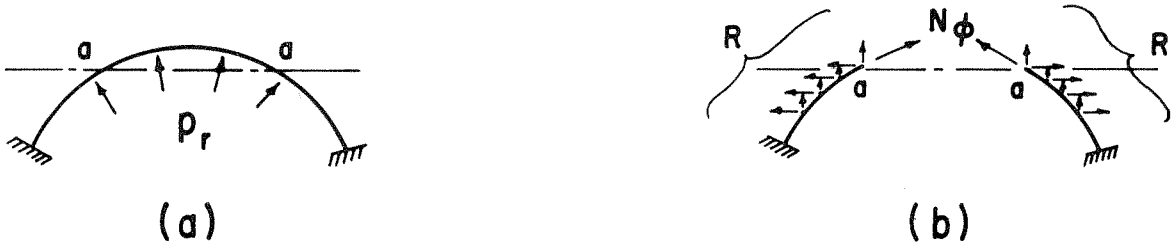

FIG. 10

Fig. 10(a) shows a spherical shell under internal pressure p_r. It is known that the portion above joint a is essentially in membrane state of stress and the membrane force N_ϕ at a can be readily determined. We can, therefore, consider the portion of the shell below a, apply N_ϕ as an additional joint load at a (Fig. 10-b) and thus, reduce the number of elementary cones which need to be considered. This procedure simplifies the solution.

b) Membrane solution plus edge-displacement effect. Fig. 11(a) shows the spherical shell subject to internal pressure p_r .

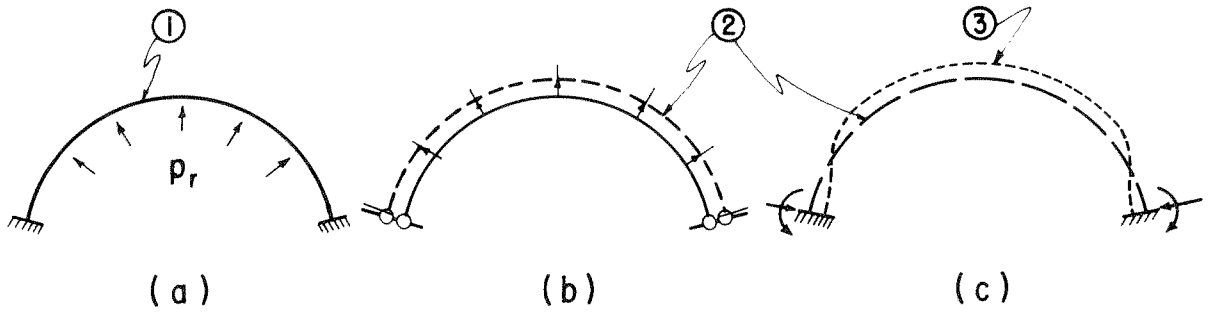

FIG. 11

We first remove the end constraints and let it deform entirely as a membrane. The shell will take the configuration shown by dashed line (2) (Figs. 11-b and 11-c). This deformed shape and the induced internal forces can be easily obtained from the membrane solution. Then we impose the known displacements at the boundary to bring the edge back to its original location and slope. At this stage bending moments and cross shears are induced in the shell, and the final configuration of the shell is shown by the dotted line (3) in Fig. 11-c. In applying this procedure, finite element analysis is used only in the last step of analysis in which only displacements at the boundary are applied. Here the problem of local moments or uneven meridianal forces around joints does not arise.

It should be remembered that the membrane solution is a convenient approximation. It represents a simplified particular solution of the governing differential equation of the shell. But for most cases, the error introduced in such an approximation is found to be negligible.

IV. APPLICATIONS OF FINITE ELEMENT SOLUTION

A. Examples 1-10

A large number of examples had been worked out in order to test the correctness of the formulations presented in the previous sections and to explore the advantages or disadvantages of each particular sequence of operations. A number of these examples will be presented in this chapter to illustrate applications of the method and to illustrate some of the difficulties encountered in solving problems.

For convenience of comparison, most of the examples involve the analysis of the same shell by different procedures. Thus, methods of using different joint loads, different number of elements, different stiffness of spherical cap, and special short-cut procedures are illustrated. Only one example is solved for a cylindrical pipe to illustrate the application of cylindrical elements.

The shell analyzed in most of the examples is a spherical one of constant thickness fixed at the bottom with a central semi-angle of 75°, a radius of 100 in. and thickness of 1/2 in., subject to an internal pressure of 100 psi. The assumed material properties are $E = 10^7$ psi and $\nu = 0.2$.

Hetényi's solution of a spherical shell[22] which is believed to be sufficiently accurate for all practical purposes is used as a basis of comparison. Rajan also formulated a solution for spherical shells[23] in closed mathematical form; the critical values of meridianal moments obtained by using this method are also listed for comparison.

Several steps are involved in solving the problem. First, decision must be made regarding the number of elements to be used to approximate the

actual shell and where the joints should be located. When the locations of the joints are selected, the geometry of the conical elements can be computed and from this the appropriate Thompson functions are obtained using certain parameters. The flexibilities and/or stiffness of the elements are then developed using these Thompson functions. Separate computer programs have been written for these purposes including the calculations of approximate joint loads. When the stiffnesses of the elements are available, one single large program takes care of all the remaining steps of the solution including the development of joint loads from fixed-edge forces if necessary. All computations are carried out by IBM 7090 computer, under the UCB Computer Center job number 255.

The criterion for judging the accuracy of a solution is a comparison with other known solutions of the distribution of the meridianal moments in general and especially of their critical values at the fixed edge. In a few cases the meridianal tension is also shown.

Ex. 1

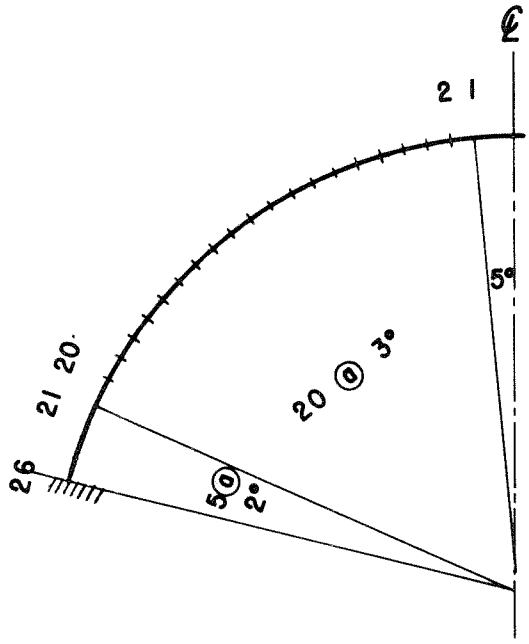

FIG. 12 - 25 CONE ARRANGEMENT OF 75° SPHERE.

The 75° sphere was analyzed as an assemblage of a 5° spherical cap and 25 cones as shown in Fig. 12. Approximate joint loads were used.

The meridianal moments M_s, membrane force N_s at each joint and the displacements Δ_h and Δ_v of each joint are tabulated below.

In the table, N_s below joint indicates the N_i force in the element below the joint, N_s above joint indicates the N_j force in the element above the joint.

For each element $N_i = \bar{r} \cdot N_j$.

Joint	∅	M_s	N_s		Δ_h	Δ_v	Joint	∅	M_s	N_s		Δ_h	Δ_v
			Above	Below						Above	Below		
1	5°	-608		6731	.0091	.0931	14	44	-113	4862	5133	.0557	.0630
2	8	-155	4215	6027	.0135	.0990	15	47	-111	4875	5117	.0588	.0602
3	11	- 85	4396	5724	.0159	.0882	16	50	-112	4887	5111	.0624	.0578
4	14	- 97	4514	5551	.0191	.0829	17	53	-134	4905	5120	.0659	.0552
5	17	-110	4595	5446	.0230	.0812	18	56	-112	4933	5109	.0671	.0510
6	20	-114	4655	5370	.0272	.0802	19	59	-107	4941	5096	.0683	.0467
7	23	-114	4701	5316	.0312	.0789	20	62	-103	4948	5084	.0706	.0433
8	26	-114	4738	5272	.0351	.0773	21	65	-104	4955	5061	.0752	.0408
9	29	-114	4767	5238	.0388	.0754	22	67	-127	4981	5054	.0761	.0381
10	32	-114	4792	5208	.0425	.0733	23	69	-165	4984	5052	.0687	.0321
11	35	-115	4813	5185	.0460	.0710	24	71	-161	4987	5045	.0495	.0220
12	38	-115	4832	5168	.0494	.0685	25	73	+ 15	4990	5042	.0197	.0091
13	41	-114	4848	5149	.0526	.0659	26	75	+544	4993		0	0

NOTE: All quantities are in inch and pound units.

Ex. 2 The same assemblage as in Ex. 1 was analyzed with joint loads derived from the fixed-edge forces of the elements. A 2 x 2 stiffness was used for the cap. The results are tabulated below.

Joint	M_s	N_s		Δ_h	Δ_v	Joint	M_s	N_s		Δ_h	Δ_v
		Above	Below					Above	Below		
1	-507		3849	.0132	.1143	14	110	5141	4870	.0552	.0629
2	- 36	6147	4216	.0148	.1029	15	111	5127	4882	.0581	.0599
3	68	5780	4408	.0165	.0898	16	111	5114	4894	.0608	.0567
4	81	5589	4526	.0195	.0841	17	113	5102	4905	.0633	.0533
5	85	5470	4607	.0232	.0821	18	116	5092	4915	.0658	.0499
6	91	5389	4666	.0272	.0808	19	119	5082	4924	.0688	.0469
7	97	5330	4711	.0311	.0793	20	110	5072	4933	.0729	.0444
8	101	5285	4747	.0349	.0775	21	59	5063	4960	.0754	.0410
9	103	5250	4776	.0386	.0755	22	-1.2	5038	4964	.0739	.0373
10	105	5220	4800	.0421	.0733	23	- 60	5034	4967	.0669	.0315
11	107	5196	4821	.0456	.0709	24	- 64	5031	4971	.0487	.0217
12	108	5175	4839	.0489	.0684	24	112	5027	4974	.0195	.0090
13	109	5157	4855	.0522	.0657	26	642	5024		0	0

Ex. 3 The same assemblage as in Ex. 1 was permitted to deflect as a membrane, then the edge was forced back to its original position and inclination.

Joint	M_s	N_s		Δ_h	Δ_v	Joint	M_s	N_s		Δ_h	Δ_v
		Above	Below					Above	Below		
1	-7.2		-53.0	.0070	.0841	14	-0.3	-1.1	-1.1	.0556	.0630
2	-3.5	-33.2	-22.8	.0112	.0846	15	-.13	-1.0	- .9	.0585	.0600
3	-0.9	-16.6	-12.7	.0153	.0840	16	-.27	- .9	- .8	.0613	.0569
4	-0.1	-10.0	- 8.1	.0194	.0831	17	-.02	- .8	- .8	.0638	.0535
5	-.05	- 6.7	- 5.6	.0234	.0819	18	+1.6	- .8	- .7	.0662	.0501
6	-.07	- 4.8	- 4.1	.0274	.0806	19	+4.8	- .7	- .7	.0688	.0468
7	-.08	- 3.6	- 3.3	.0313	.0791	20	+3.3	- .7	- .6	.0722	.0439
8	-.06	- 2.9	- 2.5	.0351	.0773	21	-22.8	- .6	- .6	.0757	.0410
9	-.05	- 2.3	- 2.1	.0388	.0754	22	-64.2	- .6	- .6	.0753	.0378
10	-.04	- 1.9	- 1.7	.0424	.0726	23	-112.8	- .6	- .6	.0681	.0318
11	-.03	- 1.6	- 1.5	.0459	.0710	24	-112.2	- .6	- .6	.0492	.0219
12	-.02	- 1.4	- 1.3	.0493	.0685	25	+63.9	- .6	- .6	.0197	.0092
13	-.01	- 1.2	- 1.2	.0525	.0658	26	+595.4	- .6		0	0

Note: 1. Add 500 #/in (the constant membrane force) to the results of bending analysis to obtain the total N_s in the shell.

2. The displacement values listed are total displacements caused by the membrane and bending displacements.

It is significant to list for the purposes of comparison the M_s values for the same shell based on Hetényi's and Rajan's solutions. The accuracy of these solutions is known to be very good.

Hetenyi's Solution

∅	M_s	∅	M_s	∅	M_s	∅	M_s
5°		26	-.00012	47	-.1101	67	-63.66
8		29	-.00044	50	-.2491	69	-112.1
11	Less than	32	-.00051	53	-.0042	71	-111.7
14		35	+.00132	56	+1.636	73	+62.44
17	10^{-4}	38	+.00706	59	+4.839	75	+589.2
20		41	+.0119	62	+3.338		
23		44	-.0110	65	-22.55		

Rajan's Solution

∅	M_s	∅	M_s	∅	M_s	∅	M_s
5°		26		47	-.1049	67	- 64.3
8		29	-.00035	50	-.2311	69	-110.5
11	Less than	32	-.00039	53	+.0253	71	-104.4
14		35	+.0012	56	+1.65	73	+ 79.8
17	10^{-4}	38	+.0063	59	+4.70	75	+616.0
20		41	+.0103	62	+2.82		
23		44	-.0118	65	-23.5		

Ex. 4

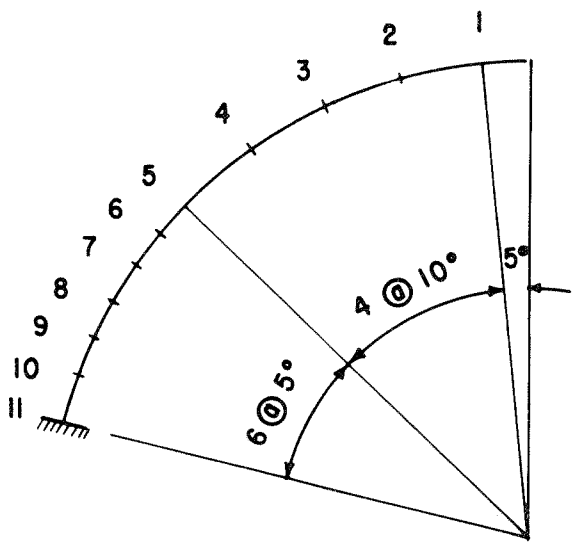

FIG. 13 - 10 CONE ARRANGEMENT

The 75° sphere as in Ex. 1 was divided into 10 cones and a 5° cap as shown in Fig. 13. The analysis was obtained by a superposing edge displacements found from the membrane solution to obtain correct boundary conditions. The meridianal moments are listed below.

Joint	M_s	Joint	M_s
1	-12	7	+ 1
2	- 2	8	+ 6
3	-.7	9	-23
4	-.4	10	-125
5	-.2	11	+594
6	-.3		

Ex. 5

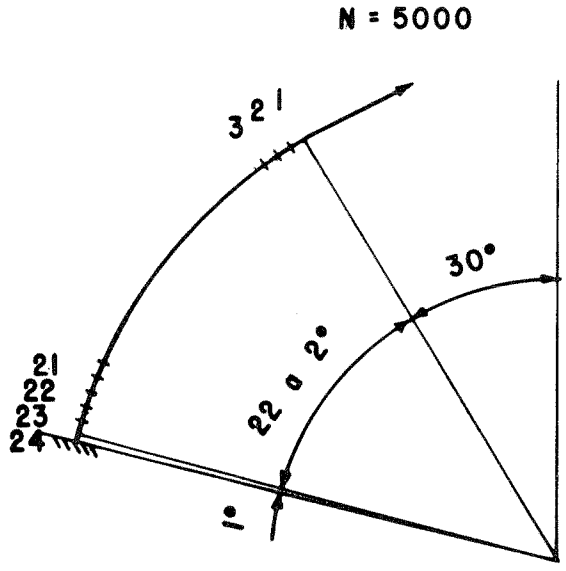

FIG. 14 - 23 CONE ARRANGEMENTS WITH CAP REPLACED BY A MEMBRANE FORCE.

The same 75° sphere as in Ex. 1. A 30° cap was removed and the remaining portion divided into 23 conical rings (Fig. 14). The force at the edge of the cap, known to be very close to membrane tension of $\frac{p_r}{2}$, is applied in the direction of the tangent of the cap. The pressure over the remaining portion of the sphere was approximated at the joints as usual. The solution yields the following meridianal moments.

Joint	ϕ	M_s	Joint	ϕ	M_s	Joint	ϕ	M_s
1	30°	0	9	46	-51.4	17	62	-47.8
2	32	-10.8	10	48	-51.2	18	64	-61.2
3	34	-31.6	11	50	-51.2	19	66	-93.1
4	36	-45.8	12	52	-51.1	20	68	-141.8
5	38	-52.0	13	54	-50.5	21	70	-175.0
6	40	-53.3	14	56	-49.2	22	72	-101.9
7	42	-52.7	15	58	-47.1	23	74	+239.0
8	44	-51.9	16	60	-45.4	24	75	+565.6

Ex. 6

The 75° sphere of Ex. 1 was divided in three different arrangements of cones, and analyzed with the approximate joint loads. The three cone arrangements are:

(1) 5° cap and 25 cones with subtended angles ranging from top to bottom of 20 of 3° and 5 of 2°. This is the arrangement used in Examples 1, 2, and 3.

(2) 5° cap and 35 cones with subtended angles of 5 of 1°, 5 of 2°, 10 of 3°, 10 of 2°, and 5 of 1°.

(3) 5° cap and 45 cones with subtended angles of 5 of 1°, 25 of 2°, and 15 of 1°.

The resulting meridianal moments for each case are plotted in Fig. 15.

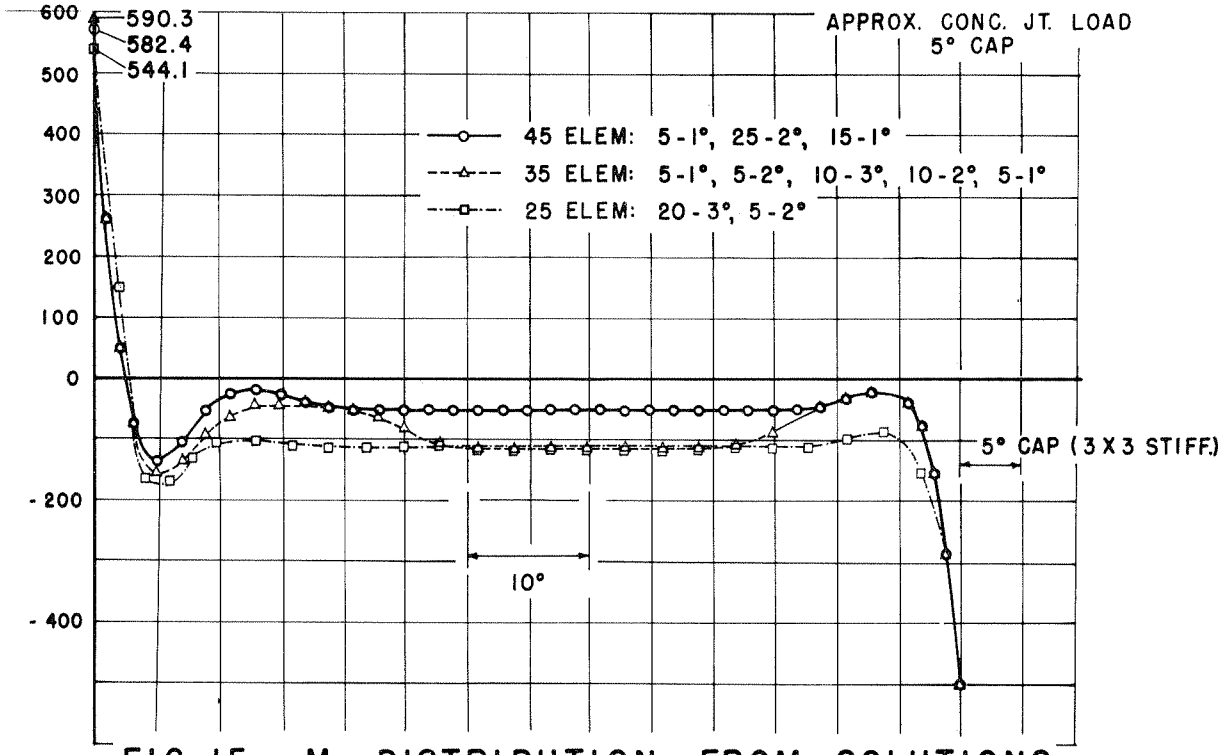

FIG. 15 M_S DISTRIBUTION FROM SOLUTIONS USING APPROXIMATE JOINT LOADS.

Ex. 7 By the same three cone arrangements as in Ex. 6, the shell was analyzed with F.E.F. joint forces. The resulting meridianal moments are plotted in Fig. 16.

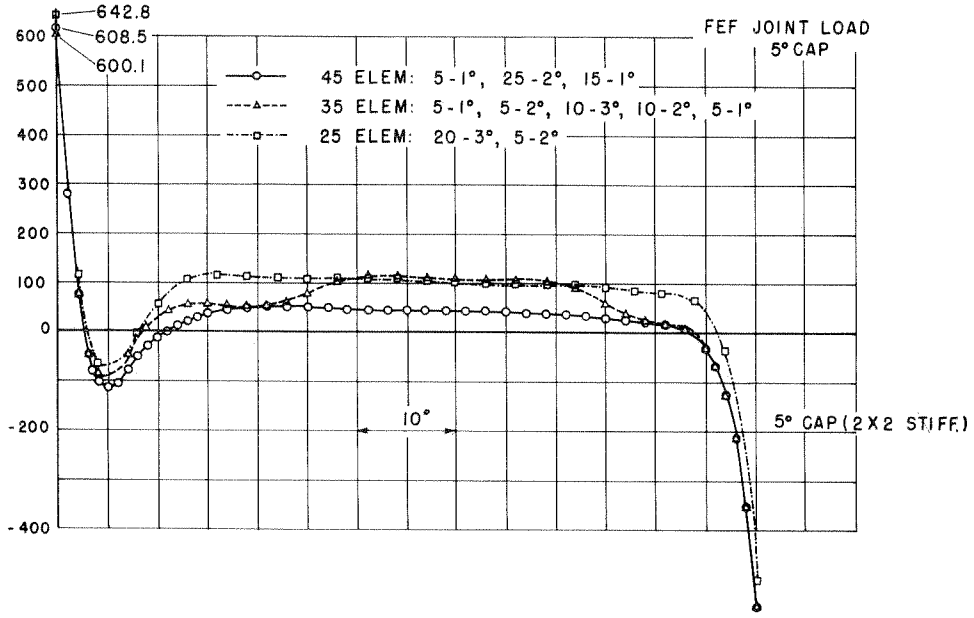

FIG. 16 M_s DISTRIBUTION FROM SOLUTIONS USING FEF JOINT LOADS.

Ex. 8 Same three cone arrangements as in Exs. 6 and 7. Superposition of edge-displacement effects on membrane solutions. The resulting M_s are plotted in Fig. 17.

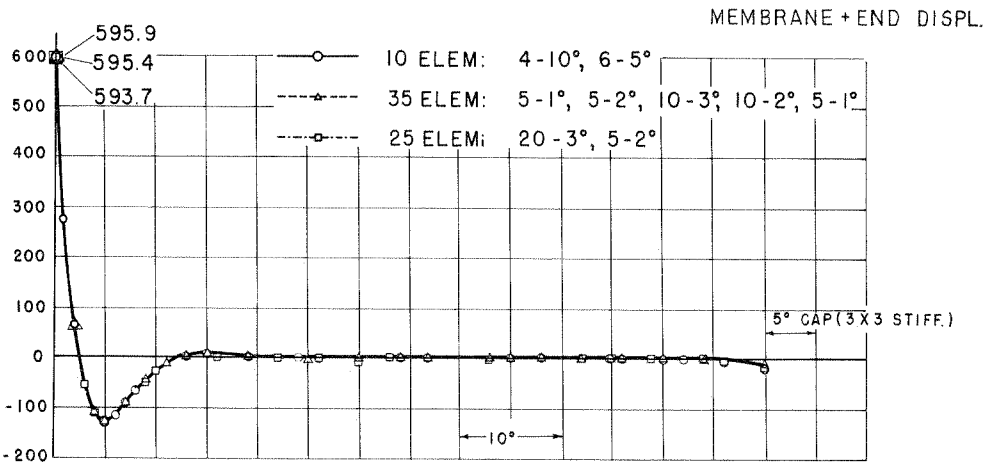

FIG. 17 M_s DISTRIBUTION - END DISPLACEMENT EFFECT

Ex. 9 The 75° sphere of Ex. 1 was analyzed with approximate joint loads using three different cone arrangements which involve uniform element lengths and break angles everywhere in the shell, except in regions next to the cap. The three cases are:

(1) 5° cap and 45 cones: 5 of 2°, 40 of $1\frac{1}{2}^{\circ}$

(2) 5° cap and 35 cones at 2° spacing

(3) 5° cap and 24 cones: 1 of 1°, 23 of 3°

The meridianal moments are plotted in Fig. 18.

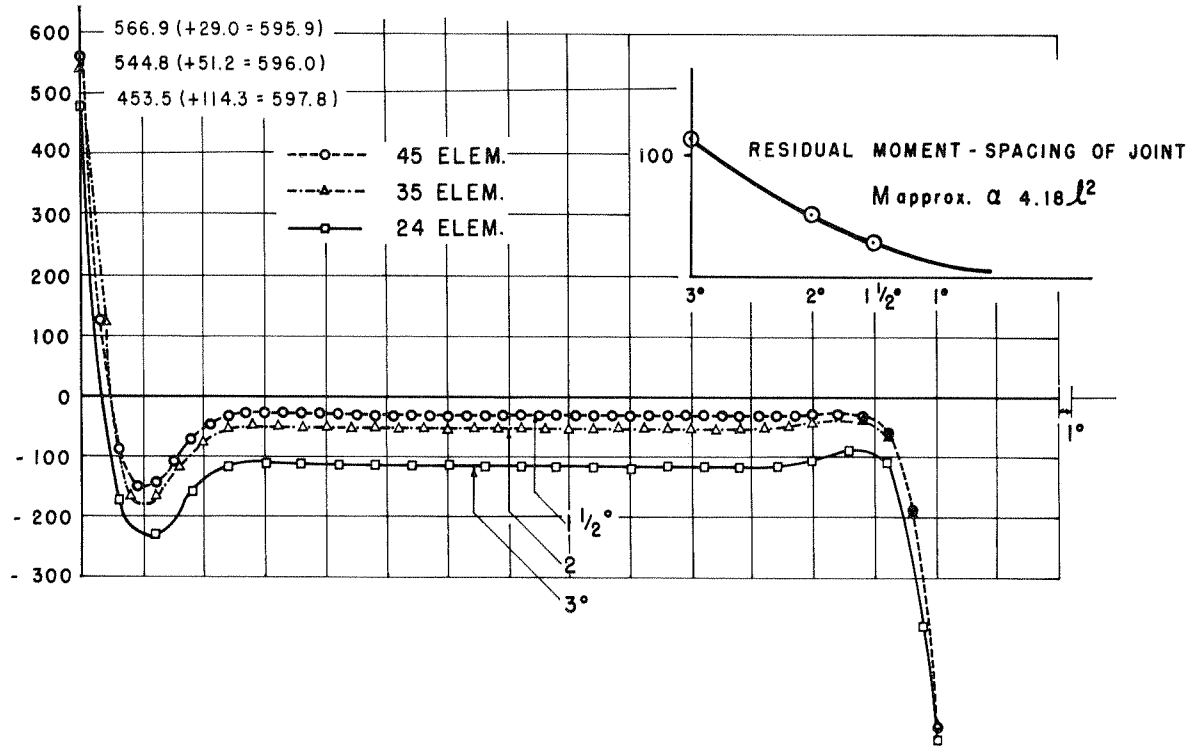

FIG. 18 M_s DISTRIBUTION FROM SOLUTIONS USING EVEN SPACING OF JOINTS.

Ex. 10

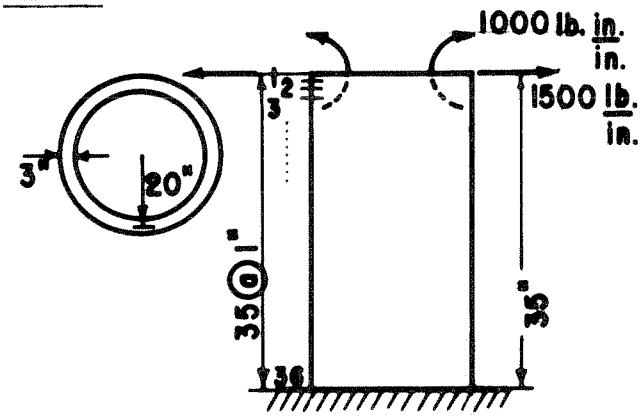

FIG. 19

A circular pipe 20" in diameter, 35" long, and 3" thick is subjected to a moment of 1000 lb-in/in and a horizontal force of 1500 lbs per in. at one end; the other end is fixed. Let $E = 3 \times 10^6$ psi, $\nu = 0$.

This problem was solved by a closed form mathematical procedure using 35 cylindrical elements of 1" length. The results of both solutions are tabulated below.

Pipe Solution by Mathematical Approach

Joint	M_x	Q	w	Joint	M_x	Q	w	Joint	M_x	Q	w
1	1000	1500	.0252	13	1083	-302	-.0018	25	-150	10	-.0002
2	2234	985	.0206	14	801	-261	-.0019	26	-138	14	-.0001
3	3003	570	.0163	15	561	-219	-.0018	27	-122	17	-.0001
4	3405	247	.0125	16	363	-178	-.0017	28	-104	18	
5	3525	5	.0091	17	204	-140	-.0016	29	- 86	19	
6	3439	-167	.0063	18	81	-107	-.0014	30	- 67	18	
7	3210	-282	.0040	19	- 11	- 78	-.0012	31	- 49	18	Less
8	2890	-350	.0021	20	- 76	- 53	-.0010	32	- 31	18	than
9	2522	-381	.0007	21	-120	- 33	-.0008	33	- 13	17	10^{-4}
10	2137	-385	-.0003	22	-145	- 18	-.0006	34	4	17	
11	1759	-369	-.0010	23	-156	- 5	-.0005	35	21	17	
12	1404	-339	-.0015	24	-157	4	-.0003	36	38	17	

Pipe Solution by Finite Element Approach

Joint	M_x	Q	w	Joint	M_x	Q	w	Joint	M_x	Q	w
1	1000	1500	.0252	13	1082	-302	-.0018	25	-150	10	-.0002
2	2234	985	.0206	14	801	-261	-.0019	26	-137	14	-.0001
3	3003	570	.0163	15	561	-218	-.0018	27	-122	17	-.0001
4	3405	247	.0125	16	363	-178	-.0017	28	-104	18	
5	3525	5	.0091	17	204	-140	-.0016	29	- 86	19	
6	3438	-167	.0063	18	81	-107	-.0014	30	- 67	18	
7	3209	-282	.0040	19	- 11	- 78	-.0012	31	- 49	18	
8	2890	-350	.0021	20	- 77	- 53	-.0010	32	- 31	18	
9	2522	-381	.0007	21	-120	- 33	-.0008	33	- 13	17	
10	2137	-385	-.0003	22	-145	- 17	-.0006	34	4	17	
11	1758	-369	-.0010	23	-156	- 5	-.0005	35	21	17	
12	1403	-339	-.0015	24	-157	4	-.0003	36	38	17	

B. Computer Programs

For an elastic analysis of shells of revolution, the following individual programs (coded originally in Fortran language) are now available.

1. Geometry and Thompson functions for conical elements.

   The argument for Thompson functions (y_i, y_j) may be very large, and the Thompson functions will involve numbers much greater than 10^{38} or smaller than 10^{-38} which are beyond the capacity of IBM 7090. Fortunately, the flexibilities of a conical element always involve the product of a ber-series function and a ker-series function. This program yields Thompson functions in which a certain positive power is taken off from all the ber-series functions while an equal negative power is taken off from the ker-series functions. These Thompson functions of false power will yield the correct flexibility matrix of a cone just as well as Thompson functions of true power.

2. Flexibility and stiffness of conical elements, good for $\alpha \leq 90^{\circ}$.

3. Thompson functions for individual numbers, good for arguments up to 120, output in true power.

4. Flexibility and stiffness of spherical cap.

   a. with singularity

   b. without singularity together with F.E.F. output

5. Flexibility and stiffness of cylindrical element (in subroutine form)

6. Approximate joint loads

7. Solution program using approximate joint loads and 3 x 3 cap stiffness, good for 45-element cone arrangement and for zero or known end-joint displacements. For other boundary conditions, it is necessary to regroup the unknowns and change the arrangements of several matrices involved.

8. Solution program using 2 x 2 cap stiffness and F.E.F. joint loads. The F.E.F. joint loads are developed within the program. The output gives the final solution (sum of fixed cones solution and the effect of unbalanced joint loads). This is good for cases with the same boundary conditions as mentioned in 7.
9. A program to compute the remaining forces (N_θ, M_θ) and stresses in the cones.

These programs will not be listed in this report but are expected to appear, possibly in slightly modified form, in a second report covering the large deformation problem.

V. CONCLUSIONS

Examples 1 and 2 of the previous chapter showed that the solutions using approximate joint loads and the F.E.F. joint loads represent two opposite trends of slow convergence. The former (using approximate loads) yields negative moments in the interior regions of the shell, and N_j values in the conical elements smaller than the known membrane force, while the N_i values are always greater than the N_j values. The latter approach (using F.E.F. joint loads) yields positive moment at interior joints and N_j values greater than the known membrane force, while the N_i values are always smaller than the N_j values. It is believed that the appearance of negative residual moments in the first approach is a natural consequence of the application of concentrated forces, and that the appearance of positive residual moment in the second approach is due to the fact that by the procedure used we have introduced some large quantities (the F.E.M.) into a region where these quantities do not exist. Since the unbalanced moment around a joint is much smaller than the fixed-end moments and the distributed moments can never exceed the unbalanced moments in magnitude, positive moments remain at the joints. However, as the number of elements becomes very large and the element lengths become small, these residual moments, positive or negative, do diminish. Examples 6 and 7 showed that the results of analysis by both approaches converge. Examples 1, 2, 3 point out the fact that the joint displacements obtained by different procedures are about same.

Example 5 illustrated the use of short-cut method by which a 23-element solution yields nearly as good results as a regular solution using 45 elements (Ex. 6).

Examples 6 and 7 showed that whenever joint loads are applied some residual moments always remain in regions where the stress condition is known to be membrane. These residual moments are positive when F.E.F. joint loads are used and negative when approximate joint loads are used. Their magnitudes depend on the lengths of the elements and the break angle between the elements. When the element lengths and break angles are made smaller, the residual moments diminish quickly ($M \propto \ell^2$). It appears that by averaging the results of a solution using approximate joint loads and those of another solution using F.E.F. joint loads, both based on the same arrangement of elements, the correct results can be obtained. Such a step, however, needs rational justification.

Examples 4 and 8 indicate the advantage of superposition of edge displacement effects on a membrane solution. By this procedure a 10-element arrangement yields nearly as good results as does a 25-element or a 35-element arrangement. No problems of residual moments arise.

Example 9 showed that when constant element lengths and break angles are used throughout (except near vertex), the M_s distribution using various element lengths all take the same shape. Their plots appear only at different heights from a base line in a graph. These different heights from the base line represent the residual moments for the particular element lengths and break angles used in the analysis. Comparing Examples 8 and 9, we see that the correct M_s distribution can be obtained by simply shifting the base line down (for approximate joint loads) and up (for F.E.F. joint loads) through an amount equal to the residual moment and read the curve referred to the new base line. But if the lengths of the elements are kept the same while the break angles are not (possible near boundaries), such an approach should not be taken because the non-uniformity

of break angles will cause local change of the slope of the M_s curve and thus impair the correctness of the result.

Example 10 simply showed the correctness and accuracy of using cylindrical elements for a solution.

We thus come to the following conclusions.

1. Finite element analysis of axi-symmetrical shells of revolution does give correct results, but due to the space nature of the problem, a much larger number of elements than that needed for a frame analysis is required for the desired accuracy.

2. The use of F.E.F. joint loads, although exact in concept, offers no practical advantage over the use of approximate joint loads. On the contrary it involves more steps for a solution than does the use of approximate joint loads.

3. For possible cases, a solution by superposition of edge-displacement effects and membrane effects is always recommended. Such a solution can make use of a relatively small number of elements and yet yield accurate results. For shells with arbitrary shape and thickness, a finite-element membrane solution is fairly simple to formulate.

4. The use of equal element lengths and equal break angles throughout the shell is recommended. In such cases a relatively small number of elements could yield correct results by the use of shifting base line approach discussed before.

5. Short-cut methods of replacing a portion of the shell with known forces can be used to save effort if possible.

6. Joint displacements are relatively insensitive to the solution method and the number of elements used.

VI. BIBLIOGRAPHY

1. Flügge, W., "Stresses in Shells", Springer, 1960.

2. Timoshenko, S., Woinowsky-Krieger, S., "Theory of Plates and Shells", McGraw-Hill, Inc., 1959.

3. Zagustin, A., Young, D. H., "On the Bending Theory of Thin Spherical Shells", to be published.

4. Rygol, J., "The Calculation of Thin Shells of Revolution of Variable Thickness", C. E. & Public Works Review, V. 55, n. 649, August 1960.

5. Kovalenko, A. D., Grigorenko, J. M., Lobkova, N. A., "Analysis of Conical Shells with Linearly Varying Thickness", U.S.S.R. Academy of Sciences, Kiev, 1961.

6. Reissner, E., "On Axisymmetrical Deformation of Thin Shells of Revolution", Proc. of Symposia in Applied Mechanics, V. 3, 1950.

7. Reissner, E., "Rotationally Symmetric Problems in the Theory of Thin Elastic Shells", Proc. of Third U. S. Congress of Applied Mechanics, June 1958.

8. Naghdi, P. M., De Silva, C. N., "On the Deformation of Elastic Shells of Revolution", QAM, V. 12, n. 4, January 1955.

9. Naghdi, P. M., De Silva, C. N., "Asymptotic Solution of a Class of Elastic Shells of Revolution with Variable Thickness", QAM, V. 15, n. 2, July 1957.

10. De Silva, C. N., "Deformation of Elastic Paraboloidal Shells of Revolution", JAM, V. 24, 1947.

11. Langer, R. E., "On the Asymptotic Solution of Ordinary Differential Equations", Trans. A. M. Soc., V. 33, 1931, V. 37, 1935.

12. Naghdi, P. M., "The Effect of Transverse Shear Deformation on the Bending of Elastic Shells of Revolution", QAM, V. 15, n. 1, April 1957.

13. Naghdi, P. M., "On the Theory of Thin Elastic Shells", QAM, V. 14, January 1957.

14. Reissner, E., "On the Theory of Thin Elastic Shells", H. Reissner Anniversary Volume, 1949.

15. Reissner, E., "Stress Strain Relations in the Theory of Thin Elastic Shells", Jour. Math. Physics, V. 31, 1952.

16. Reissner, E., "Variational Considerations for Elastic Beams and Shells", Journal ASCE, Eng. Mechanics Division, V. 88, n. 1, February 1962.

17. Green, A. E., Adkins, J. E., "Large Elastic Deformations", Oxford, 1960.

18. Argyris, J. H., Kelsey, S., "Energy Theorems and Structural Analysis", Butterworth & Co., 1960.

19. McMinn, S. J., Merchant, W., "Matrices for Structural Analysis", Wiley, 1962.

20. Jenkins, R. W., "Matrix Methods in Structural Mechanics", Nottingham, 1961.

21. Clough, R. W., Wilson, E. L., King I. P., "Large Capacity Multi-Story Frame Programs", Journal ASCE, Structural Division, V. 89, n. ST-4, August 1963.

22. Hetényi, M. I., "Beams on Elastic Foundations", University of Michigan Press, 1946.

23. Rajan, M. K. S., Penzien, J., Popov, E. P., "Analysis of Stress Concentrations in Thin Spherical Shells", I.E.R. Technical Report Series 100, Issue 22, December 1962, University of California Press, Berkeley.